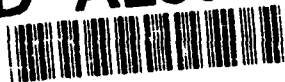


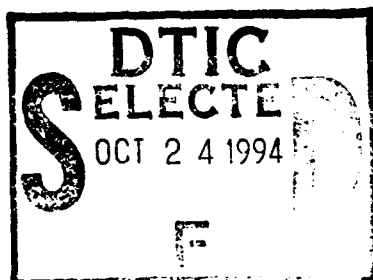
AD-A285 613



Handwritten mark

3

Technical Report 1660
April 1994



Radiance of the Ocean Horizon

C. R. Zeisse



Approved for public release; distribution is unlimited.

94-32921



REPORT DOCUMENTATION PAGE

Form Approved
OMB No. 0704-0188

Public reporting burden for this collection of information is estimated to average 1 hour per response, including the time for reviewing instructions, searching existing data sources, gathering and maintaining the data needed, and completing and reviewing the collection of information. Send comments regarding this burden estimate or any other aspect of this collection of information, including suggestions for reducing this burden, to Washington Headquarters Services, Directorate for Information Operations and Reports, 1215 Jefferson Davis Highway, Suite 1204, Arlington, VA 22202-4302, and to the Office of Management and Budget, Paperwork Reduction Project (0704-0188), Washington, DC 20503.

1. AGENCY USE ONLY (Leave blank)		2. REPORT DATE April 1994	3. REPORT TYPE AND DATES COVERED Final
4. TITLE AND SUBTITLE RADIANCE OF THE OCEAN HORIZON		5. FUNDING NUMBERS PE: 0602435N WU: DN302215	
6. AUTHOR(S) C. R. Zeisse		8. PERFORMING ORGANIZATION REPORT NUMBER TR 1660	
7. PERFORMING ORGANIZATION NAME(S) AND ADDRESS(ES) Naval Command, Control and Ocean Surveillance Center (NCCOSC) RDT&E Division San Diego, CA 92152-5000		10. SPONSORING/MONITORING AGENCY REPORT NUMBER	
9. SPONSORING/MONITORING AGENCY NAME(S) AND ADDRESS(ES) Office of Naval Research 800 N. Quincy St. Arlington, VA 22217		11. SUPPLEMENTARY NOTES	
12a. DISTRIBUTION/AVAILABILITY STATEMENT Approved for public release; distribution is unlimited.		12b. DISTRIBUTION CODE	
13. ABSTRACT (Maximum 200 words) Cox and Munk (1954) proposed that the fluctuating surface of the open ocean could be accurately represented by many small mirror-like facets, each of which is randomly tilted with respect to the local horizon. Through aerial photographs of sun glint, they determined the statistical distribution of capillary wave slopes as a function of wind velocity. However, when their equation connecting the slope distribution with sun glint is used on the horizon, an infinite glint is predicted even though it can easily be shown that sun glint should never exceed solar radiance. The objective of this report is to remove the infinite horizon radiance from the Cox-Munk model of the ocean surface.			
14. SUBJECT TERMS radiance sun glints wind speed reflection			15. NUMBER OF PAGES 99
			16. PRICE CODE
17. SECURITY CLASSIFICATION OF REPORT UNCLASSIFIED	18. SECURITY CLASSIFICATION OF THIS PAGE UNCLASSIFIED	19. SECURITY CLASSIFICATION OF ABSTRACT UNCLASSIFIED	20. LIMITATION OF ABSTRACT SAME AS REPORT

UNCLASSIFIED

21a. NAME OF RESPONSIBLE INDIVIDUAL Dr. C. R. Zeisse	21b. TELEPHONE (include Area Code) (619) 553-3602	21c. OFFICE SYMBOL Code 543

Technical Report 1660

April 1994

Radiance of the Ocean Horizon

C. R. Zeisse

Accession For	
NTIS	CRA&I <input checked="checked" type="checkbox"/>
DTIC	TAB <input type="checkbox"/>
Unclassified	<input type="checkbox"/>
Justification	
By	
Distribution/	
Avail. and/or	
Dist	Avail. and/or Special
A-1	

**NAVAL COMMAND, CONTROL AND
OCEAN SURVEILLANCE CENTER
RDT&E DIVISION
San Diego, California 92152-5001**

**K. E. EVANS, CAPT, USN
Commanding Officer**

**R. T. SHEARER
Executive Director**

ADMINISTRATIVE INFORMATION

The work in this document was performed in the Tropospheric Branch (Code 543) of the Ocean and Atmospheric Sciences Division of the Naval Command, Control and Ocean Surveillance Center RDT&E Division, San Diego, California. Sponsorship was provided by the Office of Naval Research, Washington, DC, under program element 602435N.

Released by
R. A. Paulus, Head
Tropospheric Branch

Under authority of
J. H. Richter, Head
Ocean and Atmospheric
Sciences Division

SUMMARY

OBJECTIVE

Cox and Munk (1954) proposed that the fluctuating surface of the open ocean could be accurately represented by many small mirror-like facets, each of which is randomly tilted with respect to the local horizon. Through aerial photographs of sun glint, they determined the statistical distribution of capillary wave slopes as a function of wind velocity. However, when their equation connecting the slope distribution with sun glint is used on the horizon, an infinite glint is predicted even though it can easily be shown that sun glint should never exceed solar radiance.

The objective of this report is to remove the infinite horizon radiance from the Cox-Munk model of the ocean surface.

RESULTS

An integral equation for ocean radiance is derived in this report. This equation predicts a finite radiance on the ocean horizon and the proper value of sun glint in the calm sea limit. Away from the horizon, an approximation can be used that reduces this equation to the form used by Cox and Munk. The unphysical infinity resulted from improper use of an approximation in a region where it is not valid.

CONTENTS

1. INTRODUCTION	1
2. THE GEOMETRY OF REFLECTION	3
3. THE OCCURRENCE PROBABILITY	4
4. THE INTERACTION PROBABILITY	7
5. RADIANCE REFLECTED BY A RUFFLED FOOTPRINT	12
6. TRANSFORMATION FROM OCEAN TO SKY: THE TOLERANCE ELLIPSE	15
7. SEPARATION OF RADIANCE INTO SKY REFLECTIONS AND SUN GLINTS ..	17
8. THE "FLATTOP" APPROXIMATION FOR THE GLINT RADIANCE	24
9. THE "COX-MUNK" APPROXIMATION FOR THE GLINT RADIANCE	25
10. CONCLUSION	26
11. REFERENCES	27
12. SYMBOLS	29
APPENDIX A: MATHEMATICAL DETAILS OF THE COX-MUNK-PLASS MODEL	A-1
APPENDIX B: FORTRAN SOURCE CODE LISTINGS	B-1

FIGURES

1. The geometry of facet reflection.	3
2. A plot of the occurrence probability density p as a function of slope for a windspeed of 1 m s^{-1}	4
3. A plot of the occurrence probability density p throughout slope space for a windspeed of 10 m s^{-1}	5
4. A representative facet of area dF from the pixel footprint.	6
5. The area of the ergodic cap projected toward the beam for various values of windspeed.	8
6. A plot of q versus slope for a windspeed of 10 m s^{-1} and a beam pointing toward the zenith. This figure is identical to figure 3 apart from the vertical scale.	10
7. A plot of q versus slope for a windspeed of 10 m s^{-1} and a beam pointing in the direction $\mathbf{u} = (\theta, \phi) = (80^\circ, 270^\circ)$	11
8. A plot of q in slope space for a windspeed of 10 m s^{-1} and a beam pointing in the direction $(89.75^\circ, 270^\circ)$. Only facets with positive y slopes are allowed to interact with this beam.	12
9. Instantaneous specular reflection by a single facet. The radiance of the marine sky is redirected by the facet into a receiver looking down onto the ocean surface.	13

10. The pixel footprint seen by the receiver of figure 9. Conditions are the same as for figure 7.	15
11. An expanded view of figure 7 with glint columns included.	19
12. Figure 8 showing the caps of a line of glint columns. The zenith angle of the solar center progresses from 78° to 90° in 2° steps at a fixed azimuth of 90°	20
13. Glint ratio versus solar zenith angle for a horizontal view of a sunset over a moderate sea. Parameters are the same as for figure 12 with ρ set to 100%.	21
14. Ratio of sun glint radiance leaving the footprint to solar radiance arriving at the footprint as a function of the zenith angle of the beam leaving the footprint for the receiver. Conditions: $(\theta_s, \phi_s) = (88^\circ, 90^\circ)$, $\phi_r = 270^\circ$, $W = 10 \text{ m s}^{-1}$, and $\rho = 100\%$	22
15. Ratio of glint radiance leaving the footprint to solar radiance arriving at the footprint as a function of windspeed. In this figure $(\theta_s, \phi_s) = (88^\circ, 270^\circ)$, $(\theta_r, \phi_r) = (88^\circ, 90^\circ)$, and $\rho = 100\%$	22
16. Glint pattern for a sun elevated by 2° over a moderate sea.	23
17. Glint pattern for a sun elevated by 2° over a calm sea. Except for a windspeed of 1 m s^{-1} , conditions are the same as for figure 16.	23
A-1. The reciprocal area of the ergodic cap seen by a beam as a function of that beam's zenith angle.	A-5
A-2. The ratio between the area of the ergodic cap and $A \cdot \cos \theta$ as a function of the beam zenith angle θ . The more calm the conditions the closer to the horizon the $A \cdot \cos \theta$ approximation can be used. The beam azimuth is 0°	A-6
A-3. The same as figure A-1 except for a beam azimuth of 90° . All other azimuths display deviations intermediate between these two cases of 0° and 90° azimuth.	A-6
A-4. The same as figure A-2 except for a beam azimuth of 90°	A-7
A-5. Upper figure: Coordinates for integration over the solar disk as viewed looking up at the sun from the earth. Lower figure: Spherical triangle connecting the zenith, solar center, and a position on the solar disk as viewed looking down on the sun toward the surface of the earth.	A-11

1. INTRODUCTION

Forty years ago, Cox and Munk (1954, 1956) presented a model for the fluctuating surface of the open ocean. They supposed that the sea surface consisted of numerous wave facets. Each facet is a flat surface with an area perhaps as small as a few mm². At any given instant, the ocean surface can be regarded as a collection of facets that are randomly tilted with respect to the local horizon. As time passes, the tilt of a given facet varies under the influence of the wind. When the solar disk is reflected by the open ocean, these fluctuating facets produce a dancing pattern of highlights known as sun glint.

By photographing solar reflections from an airplane, Cox and Munk were able to measure the probability

$$P \equiv p(S_x, S_y, W) dS_x dS_y, \quad (1)$$

that a wave facet would have a slope within $\pm dS_x/2$ of S_x and $\pm dS_y/2$ of S_y . S_x and S_y are the slopes of the facet in the upwind and crosswind directions respectively, and W is the windspeed. Cox and Munk obtained the following expression for the wave slope probability density:

$$p(S_x, S_y, W) \approx \frac{1}{2\pi\sigma_u\sigma_c} \exp \left\{ -\frac{1}{2} \left(\frac{S_x^2}{\sigma_u^2} + \frac{S_y^2}{\sigma_c^2} \right) \right\}$$

$$\sigma_u^2 = 0.000 + 3.16 \cdot 10^{-3} W$$

$$\sigma_c^2 = 0.003 + 1.92 \cdot 10^{-3} W. \quad (2)$$

This is actually the lowest order term of the fit found by Cox and Munk, but it will be accurate enough for our purposes. Here σ_u and σ_c are the standard deviations in the upwind and crosswind directions, respectively. Both depend on windspeed,¹ which must be entered into these expressions in m s⁻¹.

The Cox-Munk model is often cited in oceanographic literature and has proven useful in the forty years since it was first introduced. An interesting history of the Cox-Munk contribution and its relationship to earlier measurements made by Duntley was given by Preisendorfer and Mobley (1986).

The primary goal of the original Cox-Munk work was to determine the wave slope probability distribution, previously mentioned. Now that the wave slope distribution is well accepted, the concern is no longer with deriving the wave slope probability. Instead, we are interested in the

¹ A windspeed of 1 m s⁻¹ is typical of "light air: on land the wind direction is shown by smoke drift but wind vanes do not move and at sea ripples with the appearance of scales are formed, but without foam crests." A windspeed of 10 m s⁻¹ is typical of a "fresh breeze: on land small trees in leaf begin to sway and at sea there are moderate waves of 1-1/4 to 2-1/2 m height, many whitecaps, and some spray." (Bowditch, 1984).

inverse situation where, given the value of p , we wish to predict the radiance reflected from the surface of the sea. In particular, we are interested in measuring the reflected solar radiance from a low altitude, such as the deck of a ship, when the sun is anywhere in the sky, including setting; we want to look straight into a bright pattern of solar glint on the horizon and predict its radiance at a given wind velocity.

This prediction has already been provided by Cox and Munk (1954). Their equation (9) gives the radiance N leaving a glint pattern when the solar irradiance arriving at the glint pattern is H . In rearranged form and our notation, their prediction is

$$\frac{N}{H} = \frac{1}{4} \sec \theta_r \rho \sec^4 \theta_n p \quad (\text{Cox and Munk, 1954 (9)}).$$

In this equation, θ_r is the zenith angle of the reflected ray, ρ is the reflectivity of sea water, θ_n is the tilt of the facet, and p is given by equation (2). The geometry implicit in this equation is as follows: the incident ray comes from the center of the sun, the reflected ray goes to the receiver, and the facet slope is such that a specular reflection occurs between the two rays.

A problem exists with the equation (Cox and Munk, 1954 (9)) for the particular geometry in which we are interested. When viewing the horizon, θ_r approaches 90° and the radiance predicted by Cox and Munk (1954 (9)) approaches infinity. But an infinite radiance is never observed. A perfectly calm ocean (which can never occur but serves as a useful limiting case), which reflects the rays of the setting sun into a receiver mounted at the edge of the shore can be imagined. Then, any theory of solar glints should predict a radiance equal to the solar radiance times the reflectivity of sea water, because a perfectly calm ocean is exactly like a flat mirror.

This infinity is the problem addressed by this report. Three possible classes of solution are anticipated.

- (1) The theory is incomplete. The effects that have been left out are responsible for the infinity.
- (2) The theory, in particular the equation (Cox and Munk, 1954 (9)) above, is wrong. The infinity results from the error.
- (3) The theory is correct over a restricted range of conditions. The infinity results from the application of the equation (Cox and Munk, 1954 (9)) outside this range.

In returning to Cox and Munk (1954 (9)) and trying to understand its derivation, we benefited from a paper by Plass, Kattawar, and Guinn (1975), who verbally restated the geometry surrounding Cox and Munk (1954 (9)) in such a way that we could derive our own version of Cox and Munk (1954 (9)) instead. This report presents that derivation. The resolution of the unphysical infinity in Cox and Munk (1954 (9)) was discovered to reside in class (3) above.

2. THE GEOMETRY OF REFLECTION

In this report, we will only consider single scattering events as they occur at the pixel footprint. Multiple scattering and shadowing within the footprint, and transmission losses and refraction as the beams traverse the atmosphere to and from the footprint will all be ignored. Polarization will be ignored. Gravity waves will not be included.

Figure 1 shows the geometry of reflection and introduces the symbols² that will be used by this report. We have chosen a coordinate system whose origin is the point of reflection with the X axis pointing upwind, the Z axis toward the zenith, and the Y axis crosswind such that a right-handed system is formed. The X-Y plane is, therefore, horizontal at the point of reflection. The tilted facet passes through the origin. Three unit vectors $\mathbf{u} = (\theta, \phi)$ are involved in reflection. Each unit vector has polar coordinates θ , the zenith angle, and ϕ , the azimuth. Two of these unit vectors are shown in figure 1: \mathbf{u}_s , pointing from the origin to the source, and \mathbf{u}_r , pointing from the origin to the receiver. Note that the zenith angle of the facet normal (not shown) is the same as the tilt³ of the facet.

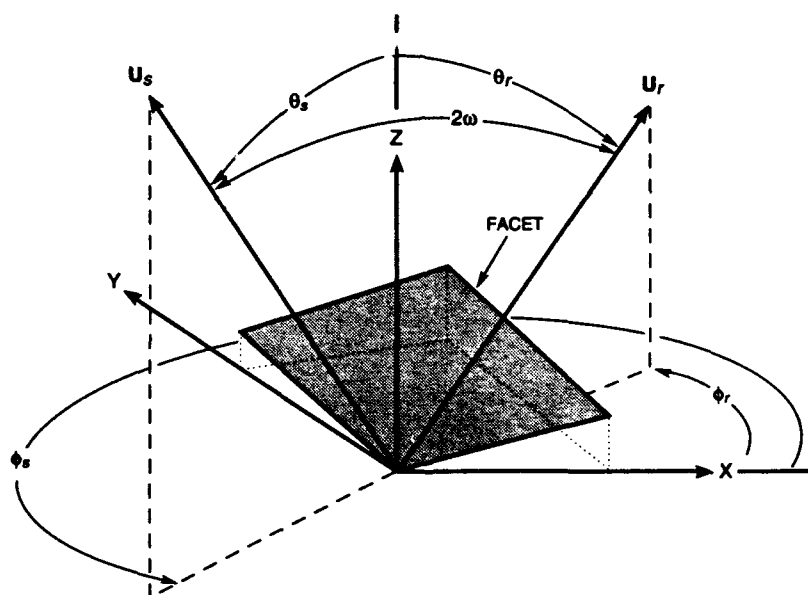


Figure 1. The geometry of facet reflection. Unit vectors \mathbf{u}_s and \mathbf{u}_r point toward the source and receiver, respectively, from the origin of a right-handed coordinate system located at the reflection point. The X axis points upwind, the Y axis points crosswind, and the Z axis points toward the zenith. The facet normal \mathbf{u}_n has been left out of the figure for clarity. Azimuths are considered positive when measured in the counterclockwise direction looking down along the nadir, a convention that conforms with mathematical usage but does not conform with nautical usage.

² The symbol list at the end of this report correlates our symbols with those used by Cox and Munk.

³ The tilt is the angle of steepest ascent within the facet.

The three vectors for source, facet normal, and receiver are connected by the law of reflection:

$$\mathbf{u}_s + \mathbf{u}_r = 2 \cos \omega \mathbf{u}_n, \quad (3)$$

where ω is the angle of incidence and the angle of reflection.

3. THE OCCURRENCE PROBABILITY

We call p the occurrence probability density because it gives the likelihood that a facet with a given slope will occur in a group of facets with all possible slopes. The shape of p is shown in figures 2 and 3 for windspeeds of 1 and 10 m s⁻¹, respectively. The volume of a column underneath p , whose base is dS_x on one side and dS_y on the other, is the probability P given by equation (1). The entire volume under the surface of p , which is the same as the integral over all slopes, is unity.

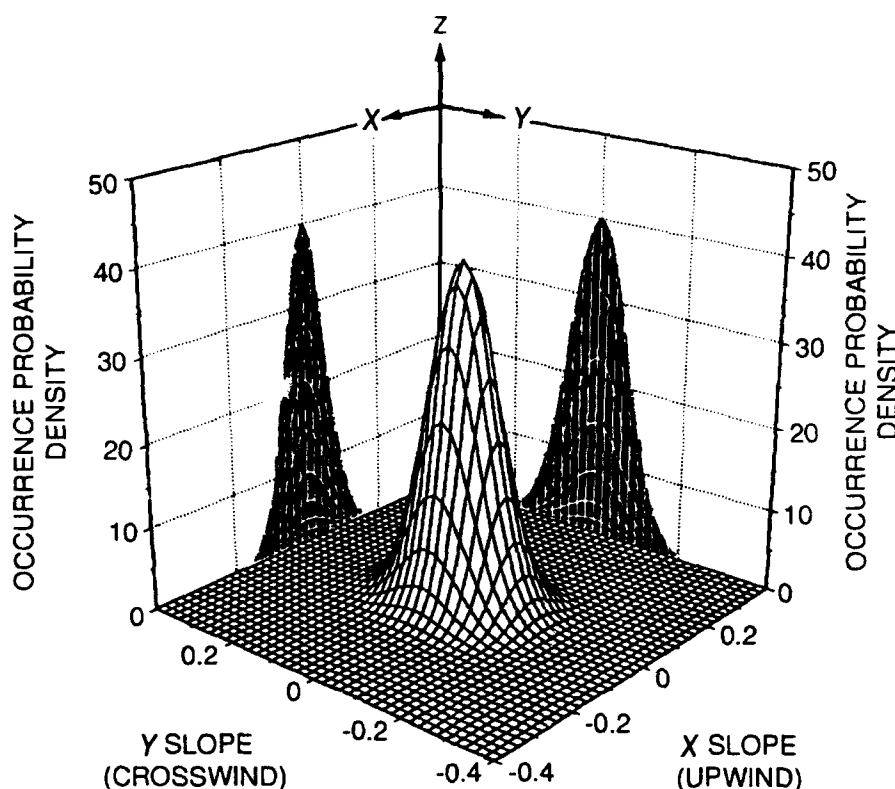


Figure 2. A plot of the occurrence probability density p as a function of slope for a windspeed of 1 m s⁻¹. In the calm sea limit, this function approaches a two-dimensional delta function selecting zero slope in each direction. The coordinate system of figure 1 has been inserted at the top of the figure to illustrate the relationship between coordinates and slopes put forth in equation (A5). Note that the first quadrant contains negative slopes.

By using the occurrence probability density, a specified area of the ocean surface can be used to represent the ocean as a whole. Let this representative piece of the ocean have an area A . Area

A can also be thought of as the footprint of a single pixel in an image of the open ocean. Within the footprint, a typical facet with area dF and tilt θ_n is shown in figure 4. Choose a convenient small range of X and Y slopes, which will be the same for all facets. Let the horizontal projection of each facet occupy an area dA whose ratio to the total area A is equal to the probability that the facet will occur:

$$\frac{dA}{A} \equiv p dS_x dS_y. \quad (4)$$

Since the occurrence probability density has been normalized to unity when integrated over all possible slopes, we have the sensible relationship that the footprint area is the sum of individual horizontal facet projections:

$$\int dA = A \iint p dS_x dS_y = A. \quad (5)$$

The collection of all facets similar to the one shown in figure 4 will represent the average condition of the wind-driven, open ocean for any chosen wind velocity. These facets can be connected together to make a continuous surface whose shape has been studied by Gordon (1969) and Preisendorfer (1976). They called this surface the "ergodic cap."

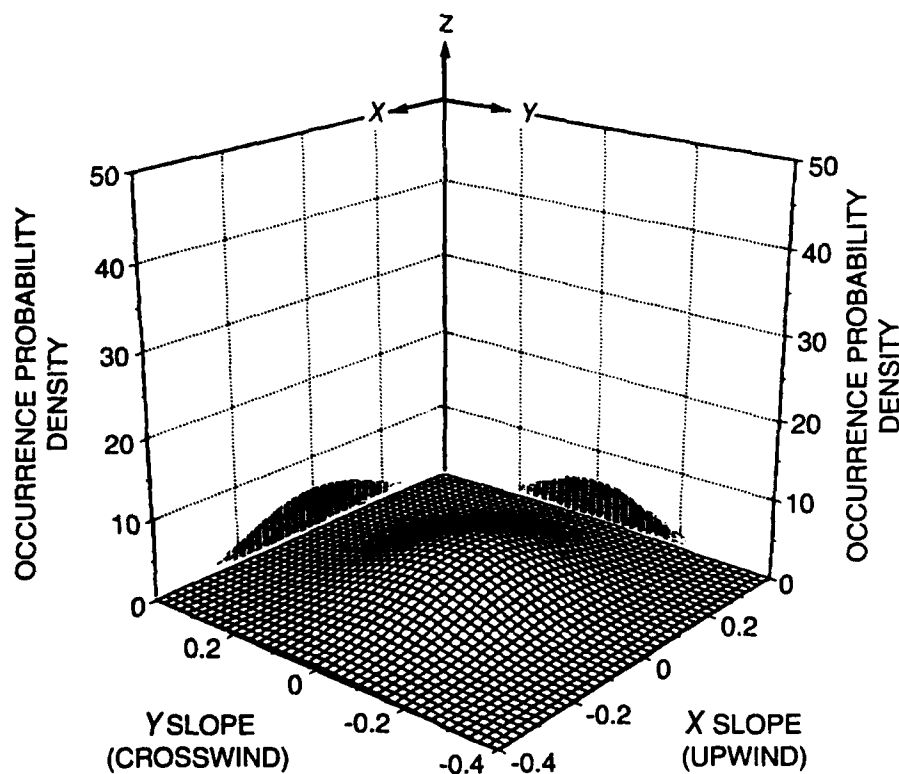


Figure 3. A plot of the occurrence probability density p throughout slope space for a windspeed of 10 m s^{-1} .

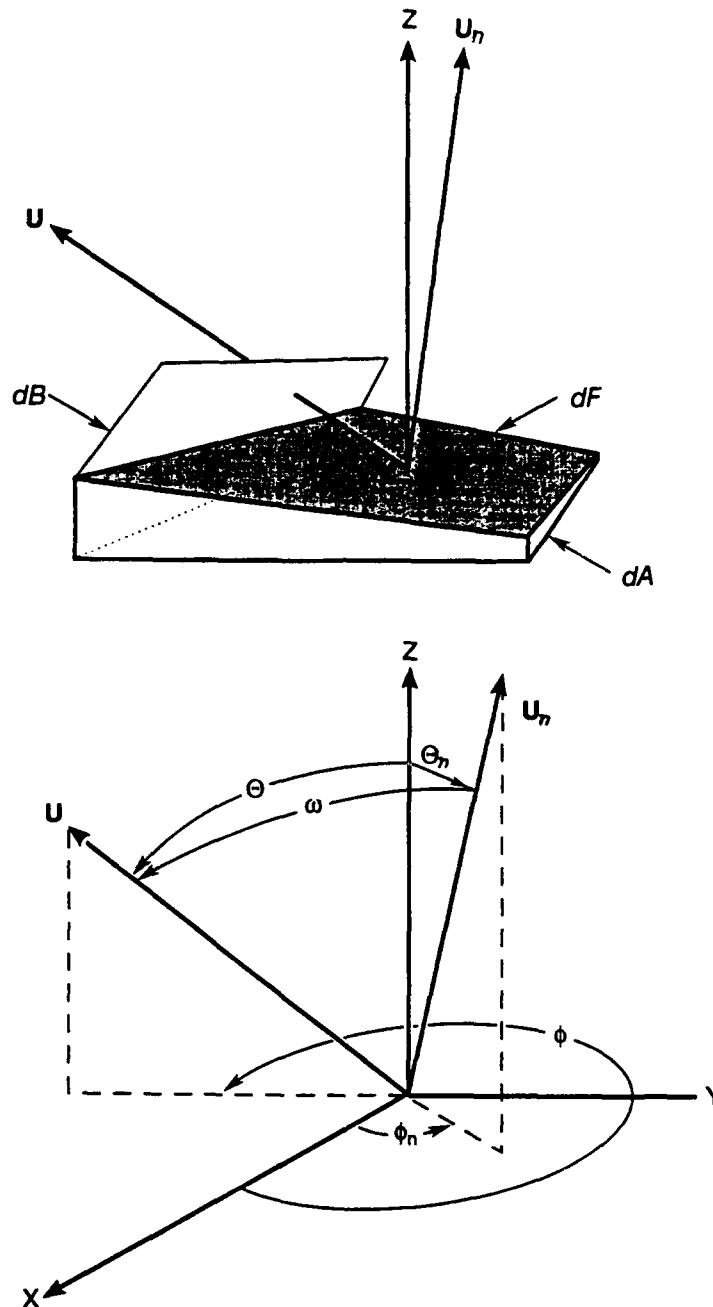


Figure 4. Upper figure: A representative facet of area dF from the pixel footprint. Its projection dA onto the horizon is proportional to the probability of finding this facet within the footprint. Its projection dB in the direction u gives the area of the facet seen from u and, hence, gives the relative importance of this facet with respect to all other facets (not shown here) that populate the footprint. Area dB is proportional to the probability this facet has of interacting with a beam toward u . Lower figure: Coordinate system for the upper figure. Unit vector u_n is normal to the facet. During the integration of equations (8), (12), and (13), u remains fixed, u_n and ω vary, and no sort of reflection is considered to occur.

4. THE INTERACTION PROBABILITY

The occurrence probability is the same as the probability that a vertical beam will interact with the facet. However, as pointed out by Plass et al. (1975), a beam that is not vertical will interact with the facet according to a different probability, which we will denote by Q and call the interaction probability. The interaction probability

$$Q \equiv q(\theta, \phi, S_x, S_y, W) dS_x dS_y \quad (6)$$

gives the chance that a beam with the arbitrary direction $\mathbf{u} = (\theta, \phi)$ will interact with a facet whose slope is within $\pm dS_x/2$ of S_x and $\pm dS_y/2$ of S_y when the windspeed is W .

We will now derive the mathematical form for q and relate it to p . The interaction probability between the beam and the facet under consideration will be proportional to the area dB of that facet projected normal to direction of the beam as shown in figure 4. Hence, by reasoning similar to that used to arrive at equation (4), we have

$$\frac{dB}{B} \equiv q dS_x dS_y \quad (7)$$

In this equation, B is the sum of all other similarly projected facets:

$$B = \int_{\substack{\omega \leq \pi/2 \\ \mathbf{u} = \text{const}}} dB \quad (8)$$

The integral of equation (8) is restricted to those facets for which the beam will strike the front rather than the back of the facet; that is, for all slopes such that $\omega \leq \pi/2$. Furthermore, the notation " $\mathbf{u} = \text{const}$ " has been added here to indicate that the beam direction is held constant during integration over the slopes.

The interaction probability can be expressed in terms of the occurrence probability because of a geometrical relationship between dB and dA evident from figure 4:

$$\begin{aligned} dB &= dF \cos \omega \\ dA &= dF \cos \theta_n \end{aligned} \quad (9)$$

Hence,

$$\frac{dB}{dA} = \frac{\cos \omega}{\cos \theta_n} \quad (10)$$

which, together with equations (4) and (7), implies that

$$q = \frac{A \cos \omega}{B \cos \theta_n} p \quad (11)$$

Equation (11) is the desired relationship between q and p . For a beam directed to the zenith, the angle of incidence is the same as the facet tilt. Then (10) shows that dB equals dA , which is

also obvious from figure 4 when \mathbf{u} points along Z . Therefore, B equals A and (11) shows that q equals p when the beam is vertical.

Using equations (7) and (11) in (8), we arrive at the following expression for the area $B(\theta, \phi, W)$ in terms of the occurrence probability:

$$\frac{B}{A} = \iint_{\substack{\omega \leq \pi/2 \\ \mathbf{u} = \text{const.}}} \frac{\cos \omega}{\cos \theta_n} p dS_x dS_y. \quad (12)$$

B must be evaluated under the exclusion of facet backs $\omega \leq \pi/2$, for each direction of the beam, and for each value of the wind velocity. The behavior of B/A for a footprint of unit area is shown in figure 5 for various wind conditions.

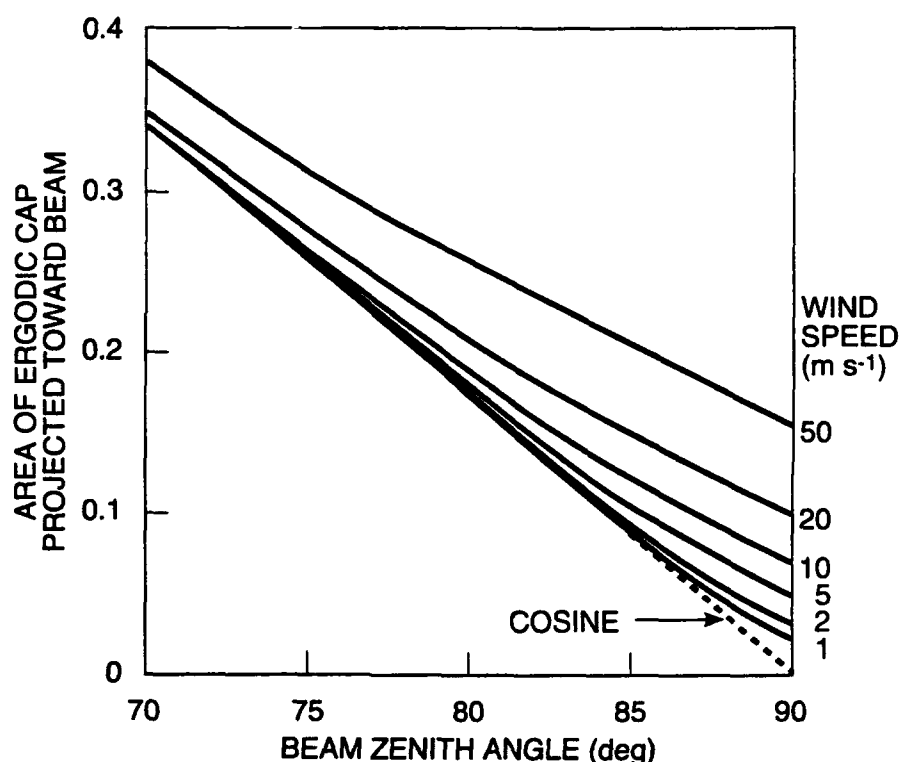


Figure 5. The area of the ergodic cap projected toward the beam for various values of windspeed. The beam is upwind (zero azimuth) and a unit area has been assumed for the footprint. The footprint contains a surface that acts rough so that it can be seen even from a glancing direction (zenith angle 90°). The greater the wind, the rougher the surface. On the other hand, the flat mirror-like surface, which represents mean sea level inside the footprint, has a projection that varies as the cosine of the beam zenith angle. It vanishes at a glancing angle.

Using (12) in (11), we have

$$q = \frac{\frac{\cos \omega}{\cos \theta_n} p}{\iint_{\substack{\omega \leq \pi/2 \\ \mathbf{u} = \text{const.}}} \frac{\cos \omega}{\cos \theta_n} p dS_x dS_y} \quad (13)$$

Equation (13) is valid for $\omega \leq \pi/2$. In the calm sea limit, $p(S_x, S_y, 0)$ approaches $\delta(S_x, S_y)$, the double integral in the denominator becomes $\cos \omega / \cos \theta_n$, and q equals p regardless of beam direction.

We emphasize that we have, thus far, considered the interaction of facets with a beam pointing in an arbitrary direction. From this point on, however, we will often be considering the situation when the beam points toward the receiver ($\mathbf{u} = \mathbf{u}_r$).

A plot of q as a function of slope is shown in figure 6 for a windspeed of 10 m s^{-1} and a beam pointing to zenith. Figure 7 shows a plot of q for a beam direction of $(80^\circ, 270^\circ)$; for example, a receiver due west of an ocean scene elevated 10° above the footprint (a receiver on the east coast of the United States looking down at the Atlantic Ocean) with the wind coming out of the south. Compared to the distribution of p whose peak is at the origin (figures 2, 3, and 6), the distribution of q is tilted so that its peak no longer occurs at the origin. Slopes with positive y values are by and large responsible for the interaction in this case because they are tilted toward the receiver. Those tilted away from the receiver (such as the one shown in figure 4) are less likely to interact with the beam (dB will be smaller) and may even be excluded (as the facet in figure 4 would be for beam elevations much lower than shown there). Figure 8 shows the distribution of q for a beam direction of $(89.75^\circ, 270^\circ)$; for example, a receiver on the shoreline of the Pacific coast looking due west with the wind coming out of the north.

As shown by (13), the volume in slope space under each of these q surfaces is unity.

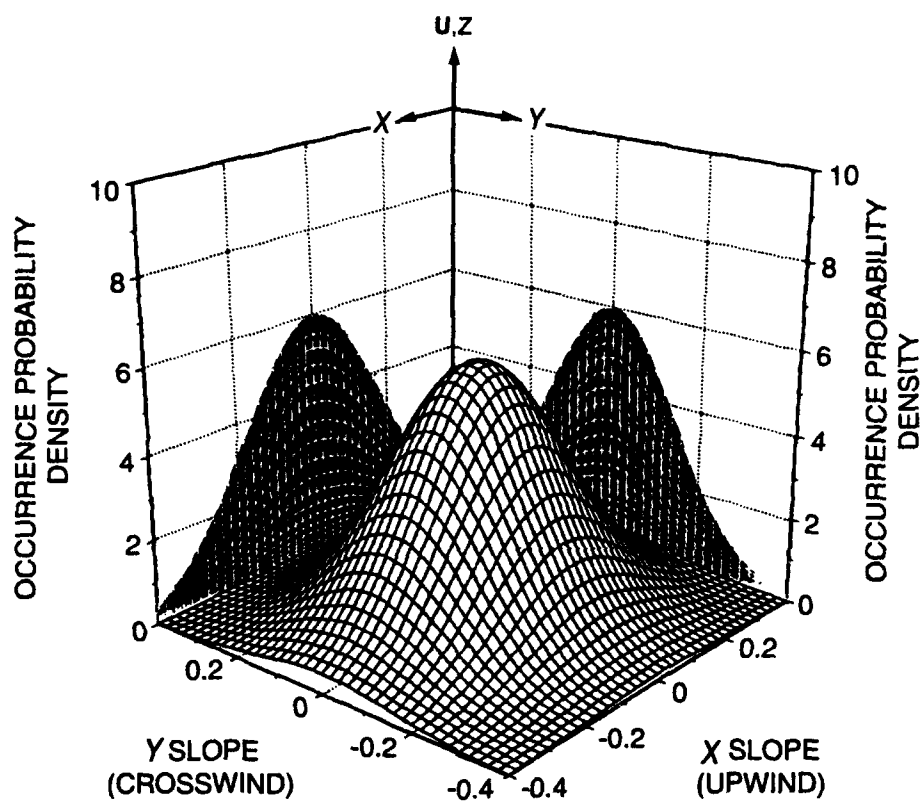


Figure 6. A plot of q versus slope for a windspeed of 10 m s^{-1} and a beam pointing toward the zenith. This figure is identical to figure 3 apart from the vertical scale.

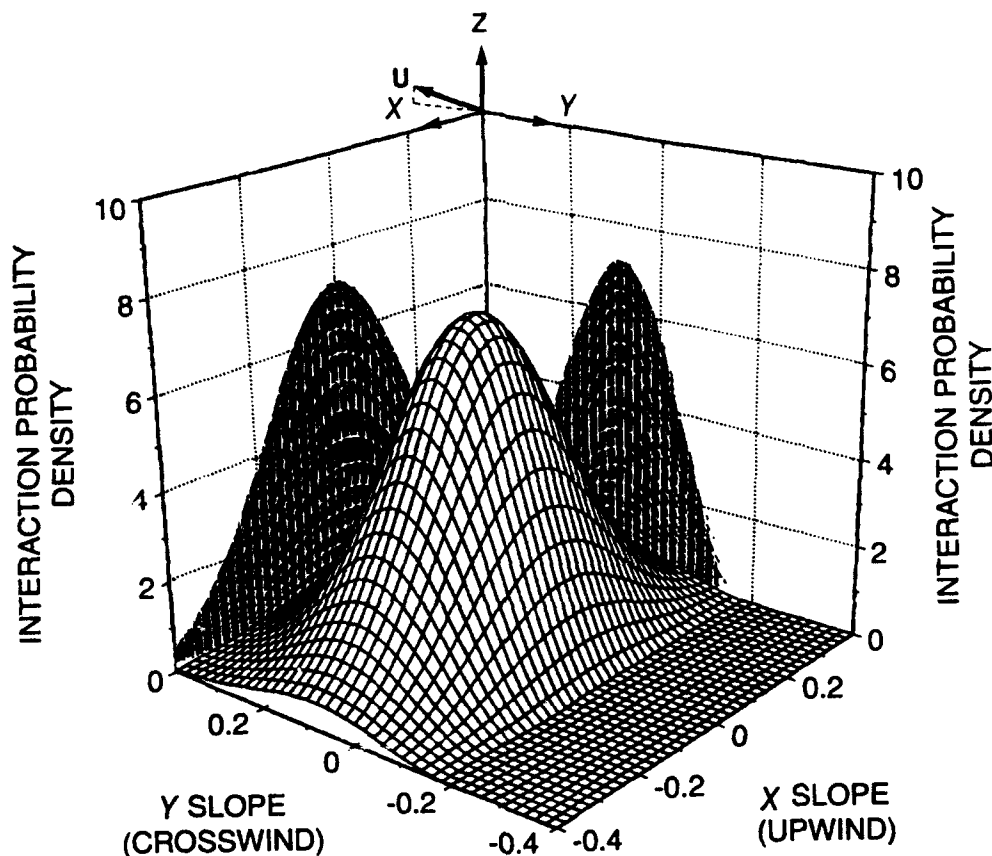


Figure 7. A plot of q versus slope for a windspeed of 10 m s^{-1} and a beam pointing in the direction $u = (\theta, \phi) = (80^\circ, 270^\circ)$. Figure 4 has been drawn for the same beam direction. Note that this distribution is tilted toward the beam direction and that slopes with large negative Y values do not interact with the beam, that is, q is zero for those slopes. This can be pictured by imagining what happens in figure 4 as the facet shown there is tilted more and more toward the Y direction: the Y slope becomes more negative, dB becomes smaller, and eventually dF contains u at a Y slope of about -0.2 whereupon the facet is parallel to the beam. Further increase in facet tilt exposes the back of the facet to the beam and by definition such facets are dropped from consideration and excluded from interacting with this particular beam.

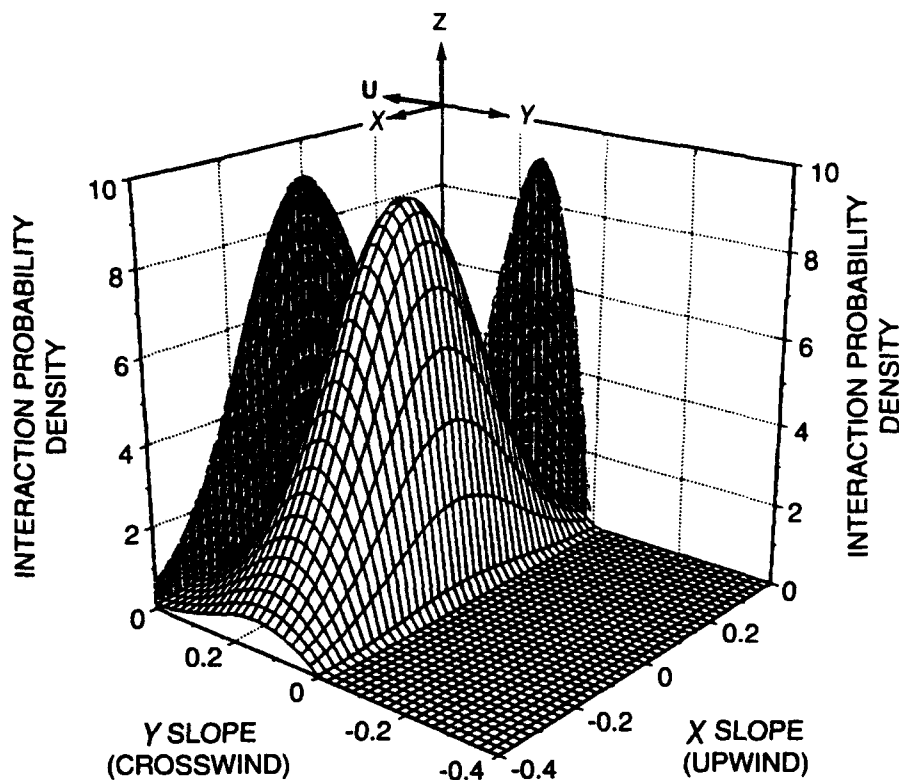


Figure 8. A plot of q in slope space for a windspeed of 10 m s^{-1} and a beam pointing in the direction $(89.75^\circ, 270^\circ)$. Only facets with positive y slopes are allowed to interact with this beam.

5. RADIANCE REFLECTED BY A RUFFLED FOOTPRINT

Having found how a beam interacts with a group of facets, we will next show how those facets reflect radiance into a receiver. Figure 9 shows the instantaneous position of a single facet whose area may be on the order of one mm^2 . The footprint area, on the other hand, is on the order of 10 m^2 after projection normal to the receiver. Therefore, figure 9 is drawn so that the facet fails to fill the receiver field of view. The situation in figure 9 is analyzed by (1) converting the radiance incident on a single facet into a power, (2) finding how the facet reflects that power, (3) adding up the reflected power from all facets within the footprint, and (4) converting the resultant sum into a radiance leaving the footprint for the receiver.

- (1) The source power arriving at the facet is contained in a beam whose radiance is N_s . If this radiance were received directly (without being altered by the facet), it would have an angular divergence of dB/R^2 at the receiver aperture where dB is the facet area projected normal to the receiver and R is the distance of the facet from the receiver. Let the area of the receiver aperture be dS . Then, from the definition of radiance as the product of the beam power per unit solid angle per unit area normal to the beam, we have

$$dP_s = N_s \frac{dB}{R^2} dS = N_s \frac{dS}{R^2} dB. \quad (14)$$

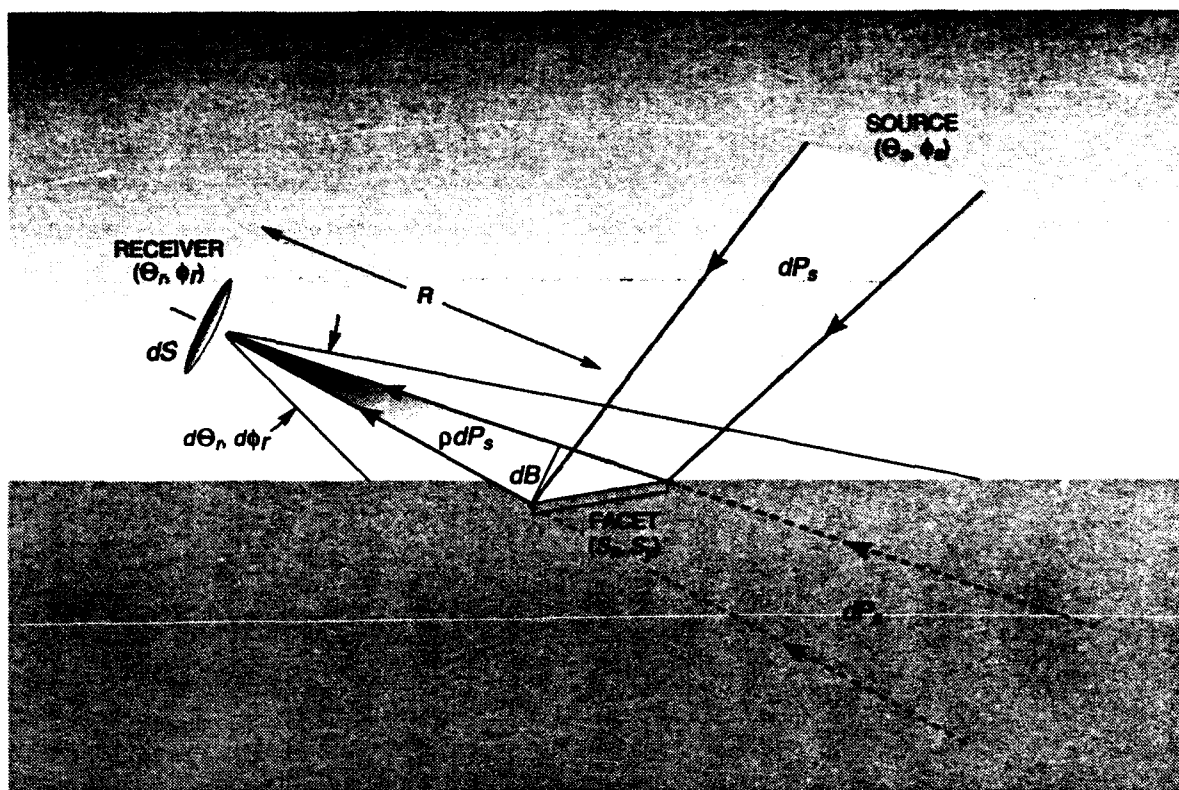


Figure 9. Instantaneous specular reflection by a single facet. The radiance of the marine sky is redirected by the facet into a receiver looking down onto the ocean surface. The power is unchanged except for a reduction due to the less than perfect reflectivity of the facet at this particular angle of incidence.

- (2) The facet reflects source power dP_s from direction \mathbf{u}_s to direction \mathbf{u}_r . After leaving the facet, this power is multiplied by the facet reflectivity ρ :

$$dP_r = \rho dP_s. \quad (15)$$

The effect of the facet mirror is simply to alter the direction of the power (as indicated by the dashed lines in figure 9) and multiply it by ρ .

- (3) The footprint, as a whole, will contain facets of all possible slopes. The power reflected from the entire footprint will be given by integration of (15) over the footprint area A :

$$P_r = \int_A dP_r = \int_A \rho N_s \frac{dS}{R^2} dB. \quad (16)$$

- (4) This total reflected power is contained in solid angle dS/R^2 and passes through area $B(\theta_r, \phi_r, W) \equiv B_r$, the area of all facets projected toward the receiver. Hence, the received radiance contributing to a single pixel is

$$N_r = \frac{P_r}{B_r \cdot (dS / R^2)}. \quad (17)$$

Substituting (16) for P_r into (17) and using (7), the received radiance can be expressed as

$$N_r = \iint_{\substack{\omega \leq \pi/2 \\ u_r = \text{const}}} \rho N_s q_r dS_x dS_y, \quad (18)$$

where the subscript on q is used as a reminder that the interaction probability density must be applied to a beam projected toward the receiver. Equation (18) shows that the interaction density q_r plays the mathematical role of a weighting factor attached to the facet position shown in figure 10.

Figure 10 shows how objects in the marine sky contribute to the radiance of a pixel in the ocean. The conditions are meant to be approximately the same as those used to draw figure 7, namely a receiver elevated by 10° and a windspeed of 10 m s^{-1} . Facets of the various slopes shown in figure 7 have captured a broad portion of the sky and redirected it toward the receiver where it is sensed as a single undivided radiance. The importance of a particular slope in the capture process is given by its weighting factor q_r in figure 7.⁴ The full-width half-maximum (FWHM) contour for the capture is elliptical, rather than circular, because the standard deviations in the upwind and crosswind directions are different.

Two comments are offered on this derivation of footprint radiance. First, we have broken the radiance apart into a power and later reassembled it into a radiance because each facet fails to fill the receiver field of view.⁵ Second, in (17), we have projected the facets (rather than the footprint) toward the receiver. This removes the unphysical infinity mentioned in the introduction because, although the footprint projects toward zero for a horizontal beam, the facets do not. The footprint is a rough surface, not a smooth one; the wind always tilts some facets so they can be seen by the receiver even though the receiver might be looking out in a direction that grazes mean sea level.⁶

⁴ Further study of the relationship between figures 7 and 10 shows that we have allowed some slopes to reflect the distant sea into the receiver, but this is incorrect. Such reflections fall into the category of multiple reflections that we have explicitly excluded. However, in the next section we will transfer our attention from integration over slopes in the sea to integration over the sky itself and then the offending slopes are conveniently excluded by integration down to, but not beyond, the horizon.

⁵ The concept of radiance invariance requires that the field of view of the detector be completely filled by the distant surface through which the conserved quantity (radiance) passes (Preisendorfer, 1976, vol II, p. 46 ff.).

⁶ Please refer to appendix A for further discussion.

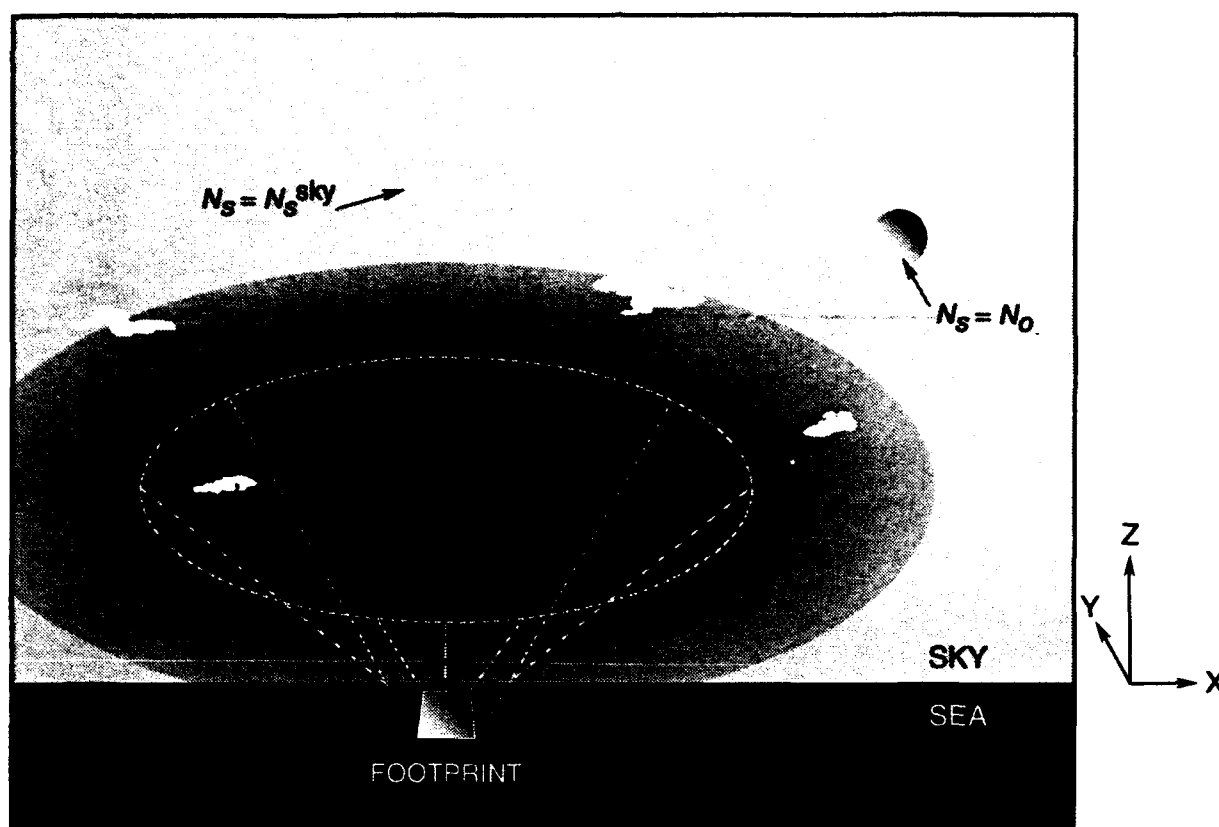


Figure 10. The pixel footprint seen by the receiver of figure 9. Conditions are the same as for figure 7. Due to the variety of slopes possessed by all the facets inside the footprint, a broad elliptical portion of the marine sky of about 10° in each direction is reflected toward the receiver where it is sensed as a single undivided radiance. The dotted line labeled "FWHM" indicates those positions in the sky that are reflected into the receiver by slopes in figure 7 for which q has the value $3\frac{1}{2}$, half its maximum value of 7.

6. TRANSFORMATION FROM OCEAN TO SKY: THE TOLERANCE ELLIPSE

Although equation (18) is the easiest way to visualize the geometry of facet reflection throughout the footprint, it is sometimes easier to integrate over objects in the sky (rather than slopes in the ocean) for the purpose of calculating the received radiance. For a fixed receiver position, the location of the source radiance in figure 9 is determined by the slope of each facet. Equations can be derived that give the sky location (θ_s, ϕ_s) reflected into a receiver located at (θ_r, ϕ_r) by a facet whose slope is (S_x, S_y) . These equations can be regarded as a transformation from slope coordinates to sky coordinates with the receiver position a parameter of the transformation. Hence, in place of equation (18), we can equally well write:

$$N_r = \iint_{u_r = \text{const}} \rho N_s q_r J d\theta_s d\phi_s, \quad (19)$$

where we have introduced the Jacobian J of the transformation between facet slope and sky position. In appendix A, it is shown that

$$J \equiv \frac{\partial(s_x, s_y)}{\partial(\theta_s, \phi_s)} = \frac{\sec \omega \sin \theta_s \sec^3 \theta_n}{4} . \quad (20)$$

The geometric meaning of this Jacobian was originally pointed out by Cox and Munk (1954) reference. The Jacobian is related to the area S of the tolerance ellipse:⁷

$$S \equiv \iint_{\text{ellipse}} dS_x dS_y = \iint_{\text{sun}} J d\theta_s d\phi_s . \quad (21)$$

The word "ellipse" under the first double integral means that the slope coordinates are restricted to the tolerance ellipse. The word "sun" under the second double integral means that the source coordinates are restricted to the solar disk. During integration over the solar disk, it is even more convenient⁸ to use a new coordinate system (ξ, χ) where ξ is the angular distance from the center of the disk, and χ is the azimuth from the upper limb of the disk.⁹ Then there will be another Jacobian J' for the transformation from sky to disk. It is shown in appendix A that

$$J' \equiv \frac{\partial(\theta_s, \phi_s)}{\partial(\xi, \chi)} = \frac{\sin \xi}{\sin \theta_s} , \quad (22)$$

so that

$$S = \iint_{\text{sun}} J J' d\xi d\chi = \iint_{\text{sun}} \sigma \sin \xi d\xi d\chi , \quad (23)$$

where

$$\sigma \equiv \frac{\sec \omega \sec^3 \theta_n}{4} . \quad (24)$$

Since the solar disk is small, σ will remain almost constant during the integration over $d\xi$ and $d\chi$ and

$$S \approx \sigma_o \iint_{\text{sun}} \sin \xi d\xi d\chi \approx \sigma_o \pi \epsilon^2 , \quad (25)$$

where ϵ is the angular radius of the solar disk and the subscript on σ means that it is to be evaluated for a ray specularly reflected from the center of the sun into the receiver.

Hence, the product of $J/\sin \theta_s$ with the area of the sun is approximately the area of the tolerance ellipse.

⁷ The tolerance ellipse contains all those slopes capable of reflecting a ray from any part of the solar disk into the receiver. The edge of the tolerance ellipse is given by equations (A12) and (A13) as the source ray negotiates the periphery of the solar disk.

⁸ For the remainder of this report, we will arbitrarily switch back and forth between integration over slopes, integration over the scene, and integration over the solar disk.

⁹ This coordinate system is shown in figure A-5.

7. SEPARATION OF RADIANCE INTO SKY REFLECTIONS AND SUN GLINTS

We now return to the calculation of the radiance received from the fluctuating surface of the wind-ruffled open ocean. Inserting equation (11) for q_r and equation (20) for J into equation (19), we arrive at the following general expression for the radiance received from the footprint:

$$N_r = \frac{1}{4} \frac{A}{B_r} \iint_{\substack{\omega \\ \mathbf{u}_r = \text{const}}} \rho(\omega) N_s(\theta_s, \phi_s) \sec^4 \theta_n p(S_x, S_y, W) \sin \theta_s d\theta_s d\phi_s. \quad (26)$$

Here, B_r is given by (12) with the beam pointing toward the receiver (that is, (12) with $\mathbf{u} = \mathbf{u}_r$) and $p(S_x, S_y, W)$ is given by (2). In equation (26), the beam from the source is specularly reflected to the receiver; therefore, ω is given by equation (A15), θ_n is given by equation (A16) or (A17), S_x is given by equation (A12), and S_y is given by equation (A13). N_r is independent of source coordinates and facet slope but still depends on sky radiance, sea water reflectivity, wind velocity, and receiver position. Equation (26) is the integral equation for the receiver radiance we have been seeking. It is an exact mathematical consequence of the Cox-Munk-Plass model for the wind-ruffled sea surface.

Next, we separate the received radiance N_r into two parts: N_r^{sky} due to the sky with the sun removed, and N_r^{sun} due to the sun alone:

$$N_r = N_r^{sky} + N_r^{sun} \quad (27)$$

$$N_r^{sky} = \iint_{\substack{\omega \\ \mathbf{u}_r = \text{const}}} \rho N_s q_r J d\theta_s d\phi_s \quad (28)$$

$$N_r^{sun} = \iint_{\substack{\omega \\ \mathbf{u}_r = \text{const}}} \rho N_s q_r J d\theta_s d\phi_s \quad (29)$$

Equation (28) gives the radiance received from the entire sky dome (with the sun removed) after reflection by the wind-roughened surface of the sea. This expression cannot be simplified further without adopting a model for $N_s(\theta_s, \phi_s)$, the sky radiance before reflection. However, if the sky radiance prior to reflection is independent of azimuth, the reflected sky radiance can be written as

$$N_r^{sky} = \frac{1}{4} \frac{A}{B_r} \int_0^{\pi/2} d\theta_s \sin \theta_s N_s(\theta_s) \int_0^{2\pi} d\phi_s \rho(\omega) \sec^4 \theta_n p(S_x, S_y, W), \quad (30)$$

where it is understood that the receiver coordinates must be held constant during these integrations.

Equation (29) gives the sun glint, the radiance received from the sun alone after reflection by the ruffled sea surface. Here, the source radiance N_s is equal to the solar radiance N_o . Since solar

radiance is constant throughout the solar disk (the sun is a Lambertian source), N_o can be brought outside the integral and we have the following equivalent expressions for the ratio of glint radiance leaving the footprint to solar radiance arriving at the footprint:¹⁰

$$\frac{N_r^{sun}}{N_o} = \iint_{\substack{\text{ellipse} \\ u_r = \text{const}}} \rho q_r dS_x dS_y \quad (31)$$

for integration over the ocean,

$$\frac{N_r^{sun}}{N_o} = \frac{1}{4} \frac{A}{B_r^{sun}} \iint_{\substack{\text{sun} \\ u_r = \text{const}}} \rho \sec^4 \theta_n p \sin \theta_s d\theta_s d\phi_s \quad (32)$$

for integration over the sky, and

$$\frac{N_r^{sun}}{N_o} = \iint_{\substack{\text{disk} \\ u_r = \text{const}}} \rho q_r \sigma \sin \xi d\xi d\chi \quad (33)$$

for integration over the sun.

In the calm sea limit, q is equal to p , p approaches a delta function selecting zero slope, and we see from (31) that

$$\frac{N_r^{sun}}{N_o} \approx \rho \quad (34)$$

as expected.

Momentarily setting the reflectivity of the sea surface to 100% for the purposes of illustration, we see that the radiance ratio in (31) is given by the volume of the interaction probability density over the tolerance ellipse. This is illustrated in figure 11. Figure 11 is an expanded view of figure 7, which was drawn for the receiver looking straight toward the sun (more precisely, for an incident azimuth of 90° and a reflected azimuth of 270°). There is one elliptical column in figure 11 for solar zenith angles of 70° , 80° , and 90° , and the location of each column within the figure is determined by the solar position. Recalling that the receiver beam zenith angle is 80° for this figure, a solar zenith angle that is also 80° requires facets with slopes close to zero for specular reflection. Hence, the column for the reflection at 80° is centered at the origin of slope space. Solar zenith angles smaller than 80° (sun higher) require facets with positive y slope for specular reflection; solar zenith angles larger than 80° (sun lower) require facets with negative y slope for specular reflection. The ratio of glint radiance leaving the footprint to solar radiance arriving at the footprint is given¹¹ by the volume of each column.

¹⁰ Recall that we are neglecting the transmission of the atmosphere so the radiance at the top of the atmosphere and at the footprint are the same.

¹¹ Ignoring the effects of reflectivity.

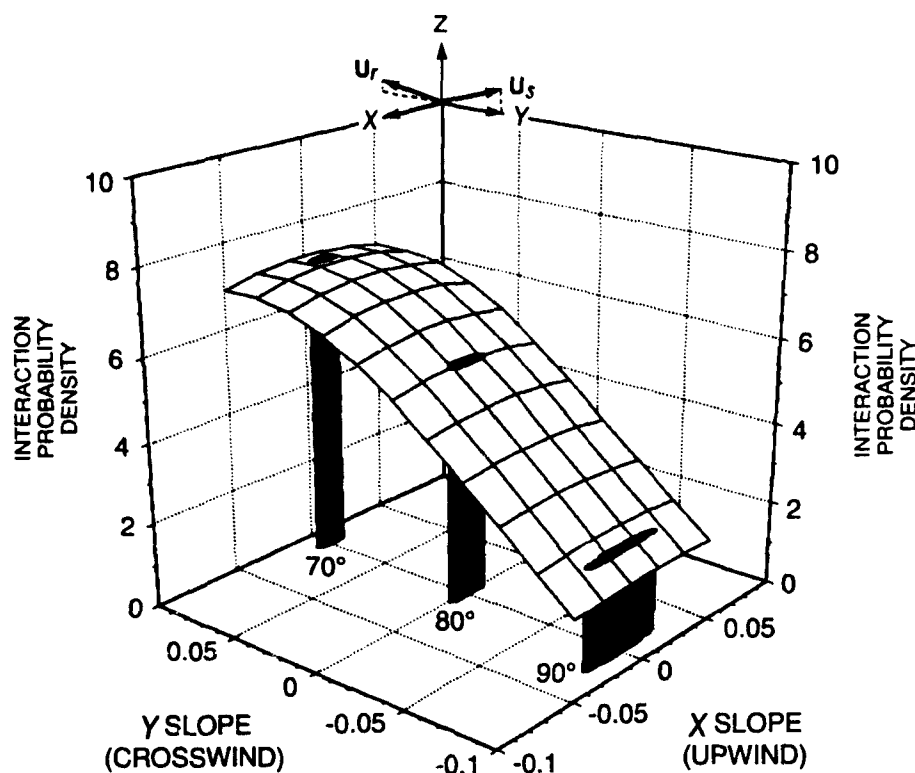


Figure 11. An expanded view of figure 7 with glint columns included. The base of each column is the tolerance ellipse and the volume (neglecting reflectivity losses) of each column is the ratio of glint radiance leaving the footprint to solar radiance arriving at the footprint. The receiver is fixed at $(80^\circ, 270^\circ)$. The solar position for each column is $(\theta_s, 90^\circ)$ where θ_s is given at the base of each column and the solar azimuth has been chosen so that the receiver is looking directly along the center of the glint pattern.

Figure 12 shows the same q surface as that shown in figure 8. In figures 8 and 12, the zenith angle of the beam leaving the footprint for the receiver is 89.75° so the received beam almost grazes the ocean surface. In figure 12, we have added crescent caps, which are the tops of each glint column for solar zenith angles stepping in 2° increments from 78° to 90° . As the sun approaches the horizon, the width of the tolerance ellipse in the Y direction remains constant, but the width in the X direction approaches infinity.¹² At the same time the position of the glint column approaches the origin of slope space where the height of the q surface becomes very small regardless of slope. Hence, even though the area of the ellipse becomes infinite (as would be expected from equation (20) for ω equal to $\pi/2$) the glint radiance ratio given by (31) remains finite for a horizontal view of the setting sun.

¹² This can be seen by imagining a receiver on the shore looking directly into a sun whose center is exactly on the far horizon. Only the upper half of the sun's disk would be visible. A facet with zero slope would be required to reflect the very top of this half-disk into the receiver, but facets with infinite slope would be required to reflect into the receiver those sides of the half-disk that touch the horizon.

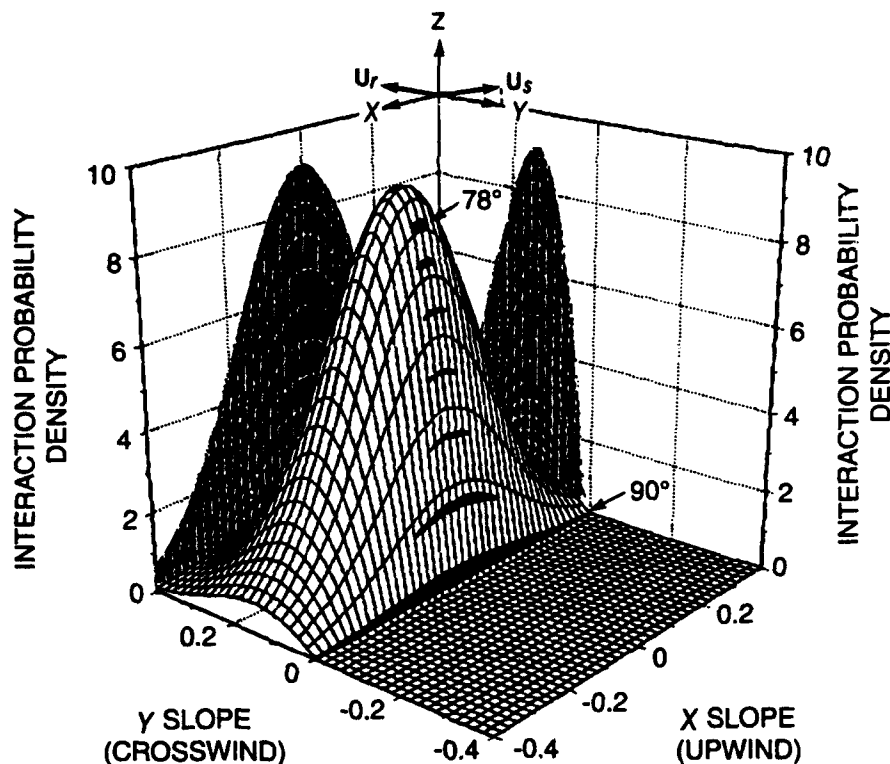


Figure 12. Figure 8 showing the caps of a line of glint columns. The zenith angle of the solar center progresses from 78° to 90° in 2° steps at a fixed azimuth of 90° . The last column occurs when both sun and receiver are very close to the horizon. It has a base that is very large (approaching ∞ in the positive and negative x directions), but it still has a finite volume since q approaches zero in those directions. The approximation associated with equation (35) amounts to the assumption that each column has a flat top.

The behavior of equations (31) through (33) for a receiver looking straight toward a setting sun is given in figures 13 through 15 by the curves labeled "Exact." Exact glint images are also shown in figures 16 and 17 for a receiver pointed into a sun elevated at 2° over moderate and calm seas, respectively. Note that the vertical scale in these figures never exceeds 2%, which may be surprising in view of the calm sea limit set forth in (34), especially for a sun setting on the horizon for which ρ approaches 100%. The exact calculations produce a smaller value than 100% because most of the slopes in a footprint deflect solar rays away from the receiver toward other parts of the sky even at very low windspeeds. In geometric terms, the volume of q_r is always much larger than the volume of a typical glint column. Put another way, the real sea always contains an appreciable number of slopes in excess of the solar radius.

We close this section with a few remarks regarding the relative strengths of the reflected sky and sun glint radiance in the visible region. The first originates in a relatively weak source, namely scattered solar radiation. The second originates in a very strong source, namely the sun itself. However, the integral in (28) for the sky covers the entire hemisphere of the sky (2π sr), whereas the integral in (29) for the glint covers only the solar disk (6.77×10^{-5} sr). The amount

of sky actually contributing to the integral in (28) will depend on how rapidly q falls off with slope. For calm conditions, a relatively small region of the sky near the specularly reflected (zero slope) receiver location will contribute to the integral. For rough conditions, many more slopes will be present and a much larger region of the sky, more like that shown in figure 10, will contribute to the integral. The point remains that the glint and reflected sky contributions can be comparable in the visible part of the spectrum even though the radiance of the sun is many orders of magnitude greater than the radiance of the sky. For example, on a clear day when the sun shines with maximum radiance, the irradiance in the visible part of the spectrum at the surface of the earth due to the sun is only about 10 times the irradiance due to the sky.¹³ On cloudy days (or in the infrared part of the spectrum where solar radiance drops by an order of magnitude), the ratio is even smaller.

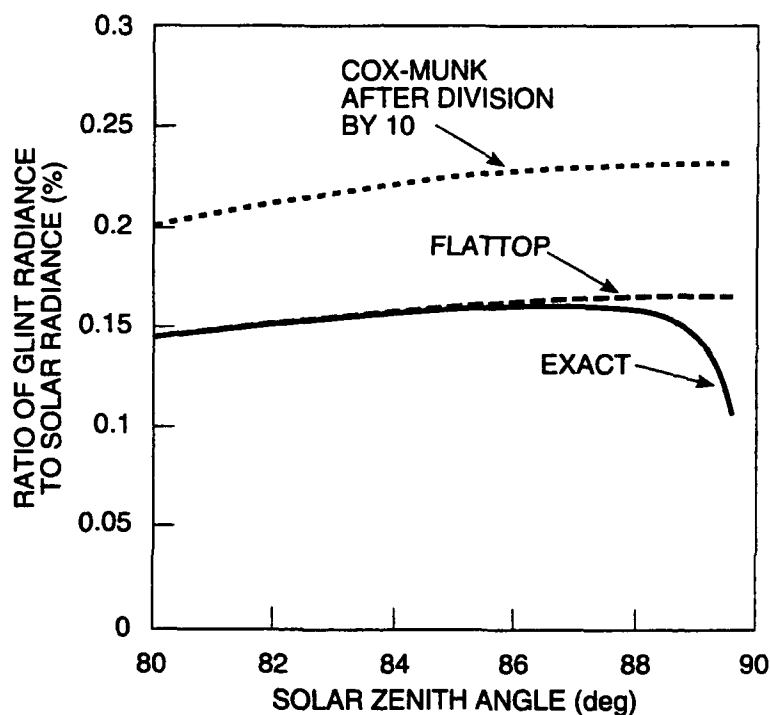


Figure 13. Glint ratio versus solar zenith angle for a horizontal view of a sunset over a moderate sea. Parameters are the same as for figure 12 with ρ set to 100%. The solid line labeled "Exact" gives the volume of the glint columns whose caps are shown in figure 12. The curves labeled "Flattop" and "Cox-Munk" show the behavior of equations (35) and Cox and Munk (1954 ((9))), respectively.

¹³ This fact was pointed out to us by Isador Halberstam, Hughes STX, Lexington, MA. Thank you, Izzy.

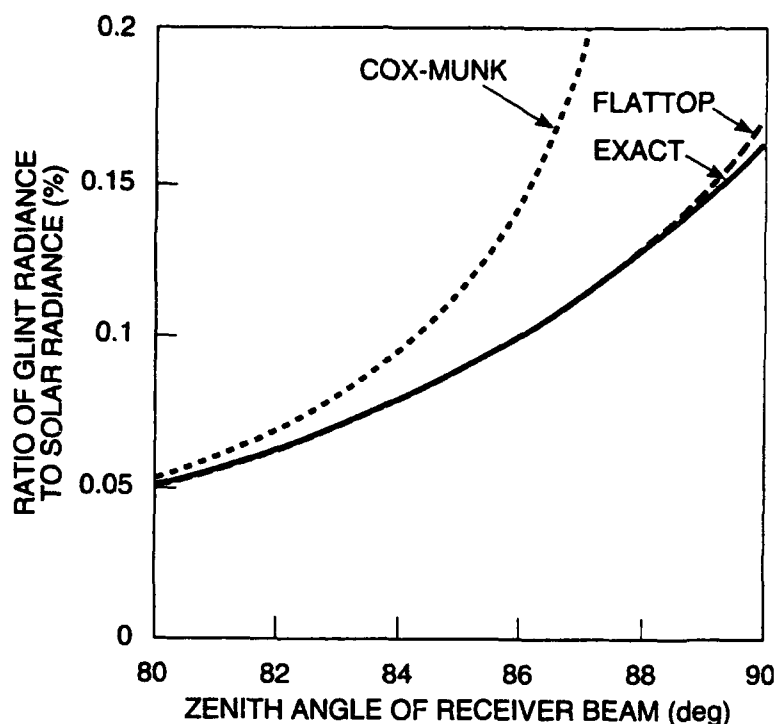


Figure 14. Ratio of sun glint radiance leaving the footprint to solar radiance arriving at the footprint as a function of the zenith angle of the beam leaving the footprint for the receiver. Conditions: $(\theta_s, \phi_s) = (88^\circ, 90^\circ)$, $\phi_r = 270^\circ$, $W = 10 \text{ m s}^{-1}$, and $\rho = 100\%$.

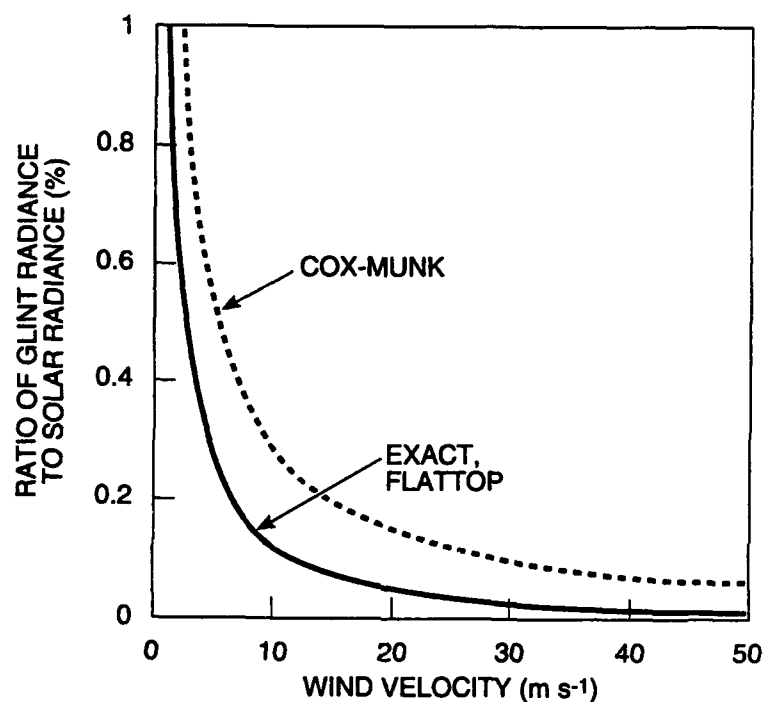


Figure 15. Ratio of glint radiance leaving the footprint to solar radiance arriving at the footprint as a function of windspeed. In this figure $(\theta_s, \phi_s) = (88^\circ, 90^\circ)$, $(\theta_r, \phi_r) = (88^\circ, 270^\circ)$, and $\rho = 100\%$.

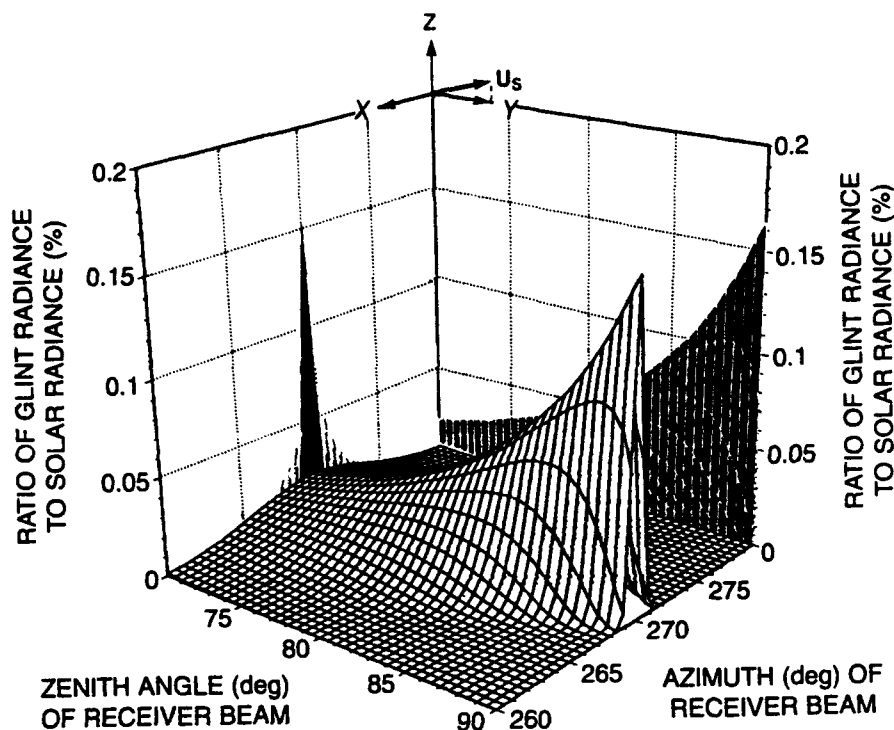


Figure 16. Glint pattern for a sun elevated by 2° over a moderate sea. The sun is to the right of the diagram, near the positive Y axis, with an azimuth of 90° . The receiver is to the left of the diagram, near the negative Y axis, looking directly toward the sun. The windspeed is 10 m s^{-1} . The reflectivity is 100%.

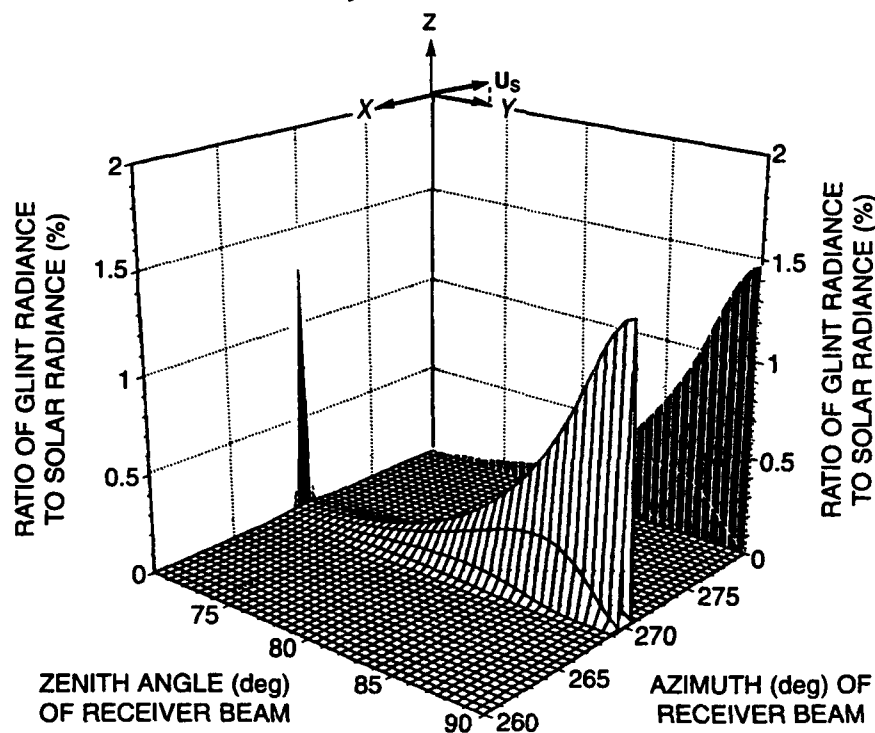


Figure 17. Glint pattern for a sun elevated by 2° over a calm sea. Except for a wind-speed of 1 m s^{-1} , conditions are the same as for figure 16. Note the change in vertical scale compared to the previous figure.

8. THE "FLATTOP" APPROXIMATION FOR THE GLINT RADIANCE

Figures 13 through 15 also contain curves marked "Flattop". These are an approximation, which will now be derived, for the exact glint expressions. The idea behind the "Flattop" approximation was used earlier without comment to obtain (25) as an approximation for the tolerance ellipse; the small size of the solar disk allows an integrand, this time the one in (31), to be brought outside an integral. Then, the ratio of glint radiance leaving the footprint to solar radiance arriving is given approximately by

$$\frac{N_r^{sun}}{N_o} \approx \{ \rho q_r \}_o \iint_{\substack{\text{ellipse} \\ \mathbf{u}_r = \text{const}}} dS_x dS_y = \{ \rho q_r \}_o \cdot S \quad (35)$$

for integration over the ocean, or

$$\begin{aligned} \frac{N_r^{sun}}{N_o} &\approx \left\{ \frac{1}{4} \frac{A}{B_r} \sec^4 \theta_n p \right\}_o \cdot \iint_{\substack{\text{sun} \\ \mathbf{u}_r = \text{const}}} \sin \theta_s d\theta_s d\phi_s \\ &= \left\{ \frac{1}{4} \frac{A}{B_r} \sec^4 \theta_n p \right\}_o \cdot \iint_{\substack{\text{disk} \\ \mathbf{u}_r = \text{const}}} \sin \xi d\xi d\chi \\ &= \left\{ \frac{1}{4} \frac{A}{B_r} \sec^4 \theta_n p \right\}_o \cdot \pi \epsilon^2 \end{aligned} \quad (36)$$

for integration over the sky.

The meaning of (35) can be appreciated by looking at figures 11 and 12. This approximation (ignoring the effects of reflectivity) amounts to replacement of the sloping column cap by a flat-top whose height is the value of q at the column center.¹⁴

This "Flattop" approximation fails when the integrand varies appreciably during integration over the solar disk, a situation which occurs when both the sun and the receiver are near the horizon. Then, the problem with the approximation can easily be seen in figure 12. As the receiver approaches the horizon with the sun also low in the sky, the width of the tolerance ellipse approaches infinity in the X direction giving rise to a substantial overestimate of the column volume when using the Flattop; the actual column height used in the exact calculation varies appreciably across the elliptical base approaching zero in the wings. As a result, when both source and receiver are near the horizon, the real volume, and the radiance it represents, is less than the approximate value given by (35). These trends are evident in figures 13 and 14.

It is obvious from a comparison of figures 2 and 3, that the "Flattop" approximation improves as the windspeed increases. Although we have not made a study of the detailed

¹⁴ The column center is the specular reflection slope for the center of the sun.

conditions under which this approximation is valid, we will note that the approximation remains finite even when evaluated for infinite¹² slopes where θ_n approaches $\pi/2$. This can be understood by referring to (36) and noting that: (1) A/Br remains finite for receivers on the horizon,¹⁵ (2) $\sec^4 \theta_n$ approaches infinity like R^4 where R is the radius in slope space to the center of the column, and (3) p falls off for large slopes like $\exp\{-R^2/\sigma^2\}$ where σ is the rms average of upwind and crosswind deviations.

9. THE "COX-MUNK" APPROXIMATION FOR THE GLINT RADIANCE

The "Cox-Munk" approximation can be introduced by noting that facets tilted by less than the beam elevation will always present their front surface to the beam. If the wind velocity is low enough that area A is almost entirely occupied by such facets, the restriction on the angle of incidence in (12) and (13) may be dropped without appreciable error, and we may write (see appendix A) that

$$\frac{B}{A} \approx \iint_{u=\text{const}} \frac{\cos \omega}{\cos \theta_n} p dS_x dS_y = \cos \theta \quad (37)$$

for an arbitrary beam, and

$$\frac{B_r}{A} \approx \cos \theta_r \quad (38)$$

for a beam pointing toward the receiver.

Substituting (38) into (36), we obtain

$$\frac{N_r^{\text{sun}}}{N_o \cdot \pi \epsilon^2} \approx \left\{ \frac{1}{4} \sec \theta_r \rho \sec^4 \theta_n p \right\}_o, \quad (39)$$

and since $N_o \cdot \pi \epsilon^2$ is equal to the solar irradiance H_o , we also have

$$\frac{N_r^{\text{sun}}}{H_o} \approx \left\{ \frac{1}{4} \sec \theta_r \rho \sec^4 \theta_n p \right\}_o \quad (40)$$

for the ratio of glint radiance leaving the ocean surface to the solar irradiance arriving at the ocean surface. Equation (40) is identical to the equation used by Cox and Munk (1954 (9)).

The "Cox-Munk" approximation is valid under the same conditions for which (38) is valid. A detailed study of those conditions is given in appendix A. In contrast to the "Flattop" approximation, the "Cox-Munk" approximation improves as the windspeed decreases; for a receiver beam elevated by 10° or more, the error is less than 10% for windspeeds below 11 m s^{-1} and less than 1% for windspeeds below $3\frac{1}{2} \text{ m s}^{-1}$.

¹⁵ Cf. figures A-1 through A-4 and the discussion are in appendix A.

10. CONCLUSION

Saunders (1968), in the spirit of the first class of solutions mentioned in the introduction, pointed out that multiple reflections and shadowing should be included in any theory of solar glints. Multiple reflections occur when the source ray bounces off of several facets before reaching the receiver. Shadowing refers to the fact that slopes on the back sides of the waves and deep in the troughs between waves are hidden from view. Each of these effects becomes more important when the source or receiver approaches the horizon. (Cox and Munk did not include either effect but were careful to take measurements when both source and receiver were near the zenith to minimize the contributions of each effect.) Saunders established upper and lower limits to the observed radiance based on multiple scattering and he included shadowing by introducing a shadowing factor. His shadowing factor, which multiplies the equation (Cox and Munk, 1954 (9)), clamps the Cox-Munk radiance to a finite value for horizontal observation of solar glints. However, we do not find that the use of Saunders' shadowing factor produces the proper radiance in the calm sea limit.

In contrast to the approach of Saunders (1968) to removing the unphysical infinity, we have followed a suggestion by Plass et al. (1975). Neglecting multiple scattering and shadowing just as Cox and Munk did, we have obtained a new integral version of Cox and Munk (1954 (9)), which is correct for all geometries. The integral version, equation (32), produces a finite glint radiance reflected horizontally by the ocean surface even when the sun is also on the horizon. Furthermore, it gives the proper radiance in the calm sea limit.

When the reflected beam is elevated by more than about 10° over a moderate sea, an approximation may be employed that reduces the exact formulation we have derived to (40), the form used by Cox and Munk. We, therefore, see that the resolution of the unphysical infinity motivating this report lies in the third solution class of the introduction. The Cox-Munk radiance equation, equation (40), is an approximation valid for radiance away from the horizon. Near the horizon, integral equation (32) should be used instead of approximate equation (40).

General equation (26), valid for all viewing geometries, will provide the proper foundation for an improved model of ocean radiance incorporating multiple scattering and shadowing.

11. REFERENCES

- Bowditch, N. 1984. American Practical Navigator, Defense Mapping Agency Hydrographic/Topographic Center Pub. No. 9, Attn: PR, Washington, DC, 20315, p. 1312.
- Cox, C., and W. Munk, 1954. "Measurement of the Roughness of the Sea Surface from Photographs of the Sun's Glitter," *Journal of the Optical Society of America*, vol. 44, p. 838.
- Cox, C., and W. Munk, 1956. "Slopes of the Sea Surface Deduced from Photographs of Sun Glitter," *Scripps Institution of Oceanography Bulletin*, vol. 6, p. 401.
- Gordon, J. 1969. "Directional Radiance (Luminance) of the Sea Surface," Scripps Institution of Oceanography Visibility Laboratory, SIO ref. 69-20.
- Plass, G., G. Kattawar, and J. Guinn, 1975. "Radiative Transfer in the Earth's Atmosphere and Ocean: Influence of Ocean Waves," *Applied Optics*, vol. 14, p. 1924.
- Preisendorfer, R. 1976. *Hydrologic Optics*. Pacific Marine Environmental Laboratory, ERL/NOAA, vol. VI, p. 263 ff. [Part of a six volume set: vol. I, Introduction, PB-259273, 218 pp., vol. II, Foundations, PB-259794, 400 pp., vol. III, Solutions, PB-259795, 256 pp., vol. IV, Imbeddings, PB-259796, 204 pp., vol. V, Properties, PB-259797, 296 pp., vol. VI, Surfaces, PB-268704, 390 pp.]
- Preisendorfer, R., and C. Mobley, 1986. "Albedos and Glitter Patterns of a Wind-Roughened Sea Surface," *Journal of Physical Oceanography*, vol. 16, p. 1293.
- Saunders, P. 1968. "Radiance of Sea and Sky in the Infrared Window 800-1200 cm^{-1} " *Journal of the Optical Society of America*, vol. 58, p. 645.

12. SYMBOLS

Notes: Column I: Cox-Munk (1954). Column II: this report, text. Column III: this report, FORTRAN source code. All symbols connected with radiation (for example radiance, irradiance, and reflectivity) stand for spectral quantities valid at a single (unspecified) wave number.

I	II	III	Latin
	A	A	Area of pixel footprint.
	a	a	X component of unit vector. Upwind.
	B	B	Area of ergodic cap projected toward beam.
	b	b	Y component of unit vector. Crosswind.
	c	c	Z component of unit vector. Zenith.
Δ_h	dA		Area of single facet projected onto horizon.
	dB		Area of single facet projected toward beam.
	H		Irradiance ($W m^{-2} [cm^{-1}]^{-1}$).
H	H_o		Solar irradiance arriving at footprint.
	J		Jacobian of transformation, slopes to sky.
	J'		Jacobian of transformation, sky to disk.
	N	N	Radiance ($W m^{-2} sr^{-1} [cm^{-1}]^{-1}$).
	N_r		Reflected radiance.
	N_r^{sky}		Reflected radiance from sky.
N	N_r^{sun}		Reflected radiance from sun.
	N_e^{sea}		Emitted radiance from sea.
	N_o	N_o	Incident radiance of sun.
	N_s		Incident radiance of source (sky or sun).
	o	o	Subscript referring to the center of the sun.
	P		Probability of facet occurrence.
	P		Beam power (W).
P	p	p	Probability density of facet occurrence.
	Q		Probability of facet-beam interaction.
	q	q	Probability density of facet-beam interaction.
	R		Radius in slope space.
	R		Distance from facet to receiver.
Δ_t	S	S	Area of tolerance ellipse.
z_x	S_x	S_x	Facet slope in x direction.
z_y	S_y	S_y	Facet slope in y direction.
	u		Unit vector.
	u_n		Unit vector normal to facet.
	u_r		Unit vector pointing to receiver.
	u_s		Unit vector pointing to source.
	W	W	Wind speed.
	X		Coordinate axis pointing upwind.

	Y		Coordinate axis pointing crosswind.
	Z		Coordinate axis pointing to zenith.
Greek			
α			Azimuth of steepest ascent.
ε	ε	Epsilon	Angular radius of solar disk.
	ν	V	Wave number (cm^{-1}).
ϕ			Solar elevation.
	ϕ	P	Azimuth of \mathbf{u} .
	ϕ_n	P_n	Azimuth of \mathbf{u}_n .
	ϕ_r	P_r	Azimuth of \mathbf{u}_r .
	ϕ_s	P_s	Azimuth of \mathbf{u}_s .
	θ	T	Zenith angle of \mathbf{u} .
β	θ_n	T_n	Zenith angle of \mathbf{u}_n . Tilt.
μ	θ_r	T_r	Zenith angle of \mathbf{u}_r .
	θ_s	T_s	Zenith angle of \mathbf{u}_s .
ρ	ρ	Rho	Reflectivity of sea water.
	σ	Sigma	Area ratio: (tolerance ellipse)/(solar disk).
σ_c	σ_c	S_c	Standard deviation of S_y .
σ_u	σ_u	S_u	Standard deviation of S_x .
ω	ω	Omega	Angle of incidence, angle of reflection.
	ω		Angle between beam and facet normal.

APPENDIX A
MATHEMATICAL DETAILS OF THE COX-MUNK-PLASS MODEL

CARTESIAN COORDINATES

The coordinate system for this report is shown in figure 1.¹ We have defined unit vectors

$$\mathbf{u} = (\theta, \phi) = (a, b, c) \quad (\text{A1})$$

Here, θ is the zenith angle of the vector, and ϕ is the azimuth of the vector. The X, Y, and Z components of the vector are a , b , and c respectively. Each of the vectors points away from the origin. Azimuths are considered positive when measured counterclockwise looking along the nadir.

By resolving polar components into vertical and horizontal components, and then by resolving the horizontal component into its X and Y components, we obtain

$$\begin{aligned} a &= \sin \theta \cos \phi \\ b &= \sin \theta \sin \phi \\ c &= \cos \theta \end{aligned} \quad (\text{A2})$$

for each vector. Subscripts attached to a unit vector are used to refer to the three vectors involved in specular reflection: the subscript will equal s when referring to the source, n when referring to the facet normal, and r when referring to the receiver.

It will be convenient to have expressions for the facet orientation in terms of $S_x \equiv \partial z / \partial x$, the facet slope in the x direction, and $S_y \equiv \partial z / \partial y$, the facet slope in the y direction. These expressions can be obtained by noting that any vector $\mathbf{r} = (x, y, z)$ within the facet is perpendicular to the facet normal:

$$\mathbf{r} \cdot \mathbf{u}_n = x a_n + y b_n + z c_n = 0, \quad (\text{A3})$$

where

$$a_n^2 + b_n^2 + c_n^2 = 1. \quad (\text{A4})$$

Equation (A3) sets the direction of the normal, and equation (A4) sets its length. By evaluating equation (A3) in the X-Z and Y-Z planes, the slopes are found to be

$$\begin{aligned} S_x &= -a_n / c_n \\ S_y &= -b_n / c_n \end{aligned} \quad (\text{A5})$$

Inserting (A5) into (A4) and using the Z component of (A2), we also have

$$S_x^2 + S_y^2 = \tan^2 \theta_n. \quad (\text{A6})$$

¹ Figures 1 through 17 and equations (1) through (40) appear in the main body of this report.

PROJECTED AREA OF THE ERGODIC CAP

If all the facets, like the one shown in figure 4, are smoothly joined together, they form a surface that Preisendorfer (1976) has called the ergodic cap. B represents the area of the ergodic cap projected in the arbitrary direction \mathbf{u} . That portion of B produced by a single facet is shown in figure 4, and an expression for B/A is given by equation (12).

We will now present an approximate expression for B/A , which is valid at low windspeeds for beams near the zenith. For low windspeeds, the occurrence probability density p is narrowly peaked about zero facet tilt; p will approach a two-dimensional delta function. Furthermore, very large slopes are required for facets that present their backs to beams near the zenith, and such large slopes are very infrequent. Hence, for calm enough conditions, very few facets will occur with their backs to any given beam, especially those beams near the zenith, and the restriction on the integral in (12) that $\omega \leq \pi/2$ can be dropped without appreciable error. In this case, we have

$$\frac{B}{A} \approx \iint_{\mathbf{u}=\text{const}} \frac{\cos \omega}{\cos \theta_n} p dS_x dS_y. \quad (\text{A7})$$

The trigonometric factors in the integrand of (A7) are

$$\begin{aligned} \frac{\cos \omega}{\cos \theta_n} &= \frac{\mathbf{u} \cdot \mathbf{u}_n}{\cos \theta_n} \\ &= \frac{aa_n + bb_n + cc_n}{c_n} \\ &= -aS_x - bS_y + c. \end{aligned} \quad (\text{A8})$$

When (A8) is inserted into (A7), the beam factors (those involving a , b , and c) can be brought outside the integral since they do not depend on the facet slope. Using the facts that (1) p is even, (2) S_x and S_y are both odd, and (3) p is normalized to unity, the first two terms in (A8) vanish altogether and the last term in (A8) survives integration intact. Hence,

$$\frac{B}{A} \approx \iint_{\mathbf{u}=\text{const}} \frac{\cos \omega}{\cos \theta_n} p dS_x dS_y = c = \cos \theta \quad (\text{A9})$$

for the approximate area of the ergodic cap projected in the arbitrary direction \mathbf{u} .

Figure A-1 shows how A/B , the reciprocal projected area of the ergodic cap, behaves when projected anywhere in the sky near the horizon. In this region, the approximation just derived begins to fail. For zenith angles greater than about 80° , A/B departs from $\sec \theta$ by an amount that depends on windspeed. The higher the windspeed, the larger the deviation from $\sec \theta$. Physically, this is because the wind tilts the facets away from their calm horizontal orientation in all directions. Some are tilted away from a beam that grazes the mean surface of the sea; these facets cannot reflect and are ignored in the integral. Some facets are tilted toward the grazing beam; these facets project more area toward the beam, are more effective reflectors than if they were

horizontal, and contribute more to the integral. The net result is that a wind-ruffled ocean surface projects a finite area (rather than a zero area) horizontally. This fact is responsible for many simple observations such as the very existence of the visual horizon (Cox and Munk, 1955) and the absence of reflections of low-lying distant land masses (Minnaert, 1954).

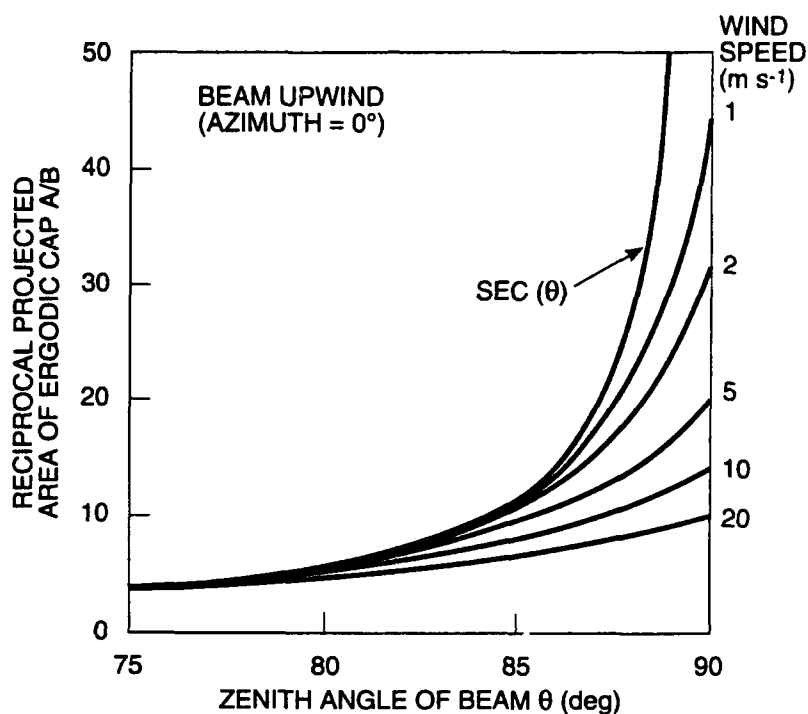


Figure A-1. The reciprocal area of the ergodic cap seen by a beam as a function of that beam's zenith angle. For zenith angles less than about 80° the secant of the zenith angle may be used for this reciprocal area to a fair approximation. For beams closer to the horizon, however, the true values deviate from the $\sec\theta$ approximation, as shown in this figure, with larger deviations at larger windspeeds. The beam azimuth is 0° .

Figure A-2 gives the same information as figure A-1 in a different form: it shows how the ratio of B to $A \cdot \cos\theta$ behaves near the horizon and is useful in estimating the accuracy of (A9) for various zenith angles and windspeeds.

Figures A-1 and A-2 have been for a beam azimuth of 0° . Figures A-3 and A-4 show the same results for a beam azimuth of 90° . For a given windspeed, results for all other azimuths are intermediate to the results given by these two cases.

Finally, we note that for beams with zenith angles less than 80° and any azimuth whatsoever, the error involved in the approximation given by (A9) is less than 1% for windspeeds below $3\frac{1}{2} \text{ m s}^{-1}$ and less than 10% for windspeeds below 11 m s^{-1} .

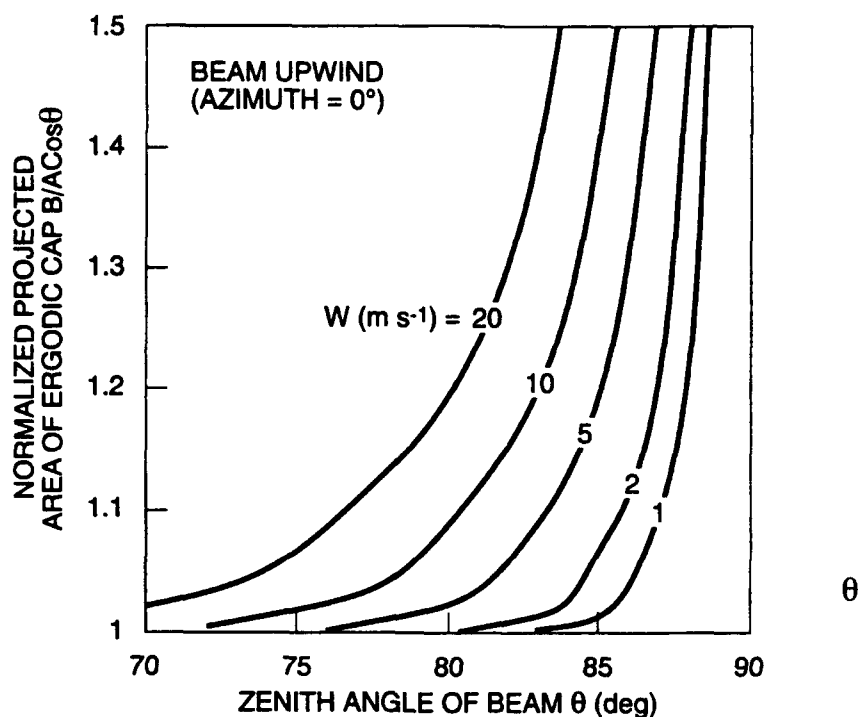


Figure A-2. The ratio between the area of the ergodic cap and $A \cdot \cos \theta$ as a function of the beam zenith angle θ . The more calm the conditions the closer to the horizon the $A \cdot \cos \theta$ approximation can be used. The beam azimuth is 0° .

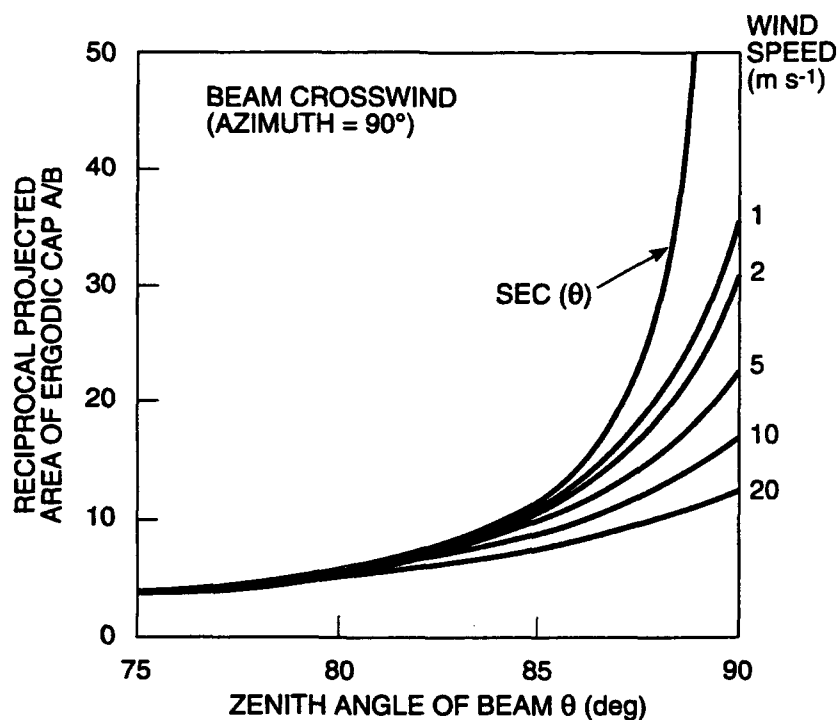


Figure A-3. The same as figure A-1 except for a beam azimuth of 90° . All other azimuths display deviations intermediate between these two cases of 0° and 90° azimuth.

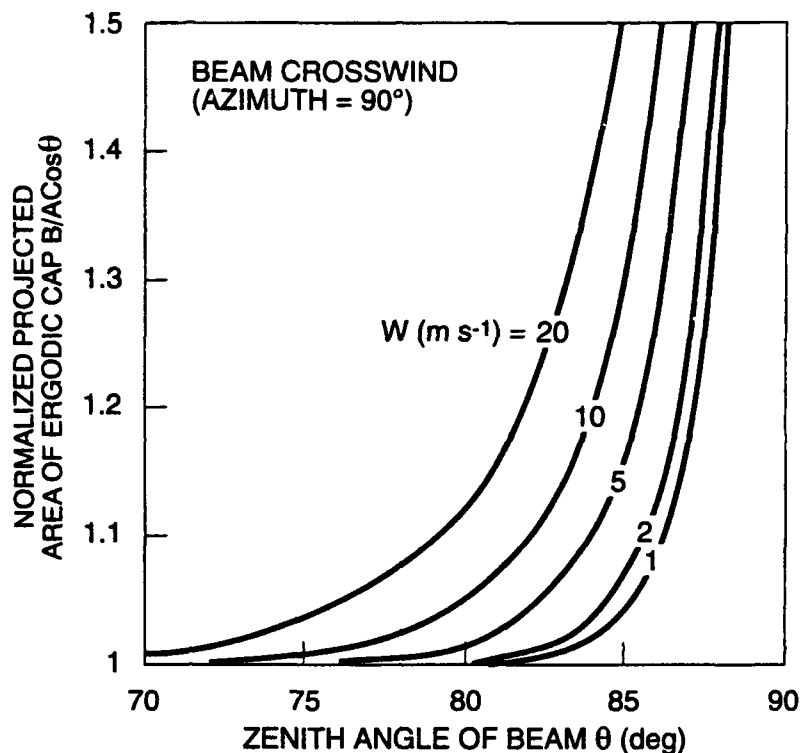


Figure A-4. The same as figure A-2 except for a beam azimuth of 90°.

APPROXIMATE EXPRESSION FOR THE INTERACTION PROBABILITY DENSITY

When the beam vector \mathbf{u} points toward a receiver well above the horizon and the wind velocity is small, $B/A \approx \cos\theta_r$. Then the interaction probability density in equation (11) can be approximated by

$$q \approx \frac{\cos\omega}{\cos\theta_r \cos\theta_n} p. \quad (A10)$$

FACET GEOMETRY FOR SPECULAR REFLECTION

For fixed positions of the source and receiver, the law of reflection

$$\mathbf{u}_n = (\mathbf{u}_s + \mathbf{u}_r) / (2 \cos\omega) \quad (A11)$$

will determine the facet position for a specular reflection between source and receiver.

We require equations for the geometry of the facet (slopes, angle of incidence, and tilt) in terms of the source and receiver coordinates. To find S_x and S_y , we can write

$$\begin{aligned} S_x &= -\frac{a_n}{c_n} = -\frac{(a_s + a_r)}{(c_s + c_r)} \\ &= -\frac{(\sin \theta_s \cos \phi_s + \sin \theta_r \cos \phi_r)}{(\cos \theta_s + \cos \theta_r)} \end{aligned} \quad (A12)$$

$$\begin{aligned} S_y &= -\frac{b_n}{c_n} = -\frac{(b_s + b_r)}{(c_s + c_r)} \\ &= -\frac{(\sin \theta_s \sin \phi_s + \sin \theta_r \sin \phi_r)}{(\cos \theta_s + \cos \theta_r)} . \end{aligned} \quad (A13)$$

The angle of incidence can be found by squaring equation (A11) to obtain

$$2 \cos^2 \omega = 1 + \mathbf{u}_s \cdot \mathbf{u}_r . \quad (A14)$$

Substituting Cartesian coordinates for source and receiver gives the following expression for the angle of incidence in terms of source and receiver positions:

$$2 \cos^2 \omega = 1 + \sin \theta_s \sin \theta_r \cos(\phi_s - \phi_r) + \cos \theta_s \cos \theta_r . \quad (A15)$$

Equations (A12) and (A13) can be substituted directly into equation (A6) to derive this expression for the tilt

$$\tan^2 \theta_n = \frac{\sin^2 \theta_s + \sin^2 \theta_r + 2 \sin \theta_s \sin \theta_r \cos(\phi_s - \phi_r)}{(\cos \theta_s + \cos \theta_r)^2} , \quad (A16)$$

and a second expression for the tilt can be found directly from the z component of equation (A11):

$$\cos \theta_n = (\cos \theta_s + \cos \theta_r) / 2 \cos \omega . \quad (A17)$$

We reemphasize that equations (A11) through (A17) apply only in case a ray from the source is reflected by the facet toward the receiver.

THE JACOBIAN FOR THE TRANSFORMATION BETWEEN OCEAN AND SKY

Equations (A12) and (A13) formally express a mathematical transformation between source coordinates in the sky and slope coordinates in the sea, if the receiver position is regarded as a parameter of the transformation. The Jacobian of the transformation is

$$J = \frac{\partial (S_x, S_y)}{\partial (\theta_s, \phi_s)} \equiv \begin{vmatrix} \partial S_x / \partial \theta_s & \partial S_x / \partial \phi_s \\ \partial S_y / \partial \theta_s & \partial S_y / \partial \phi_s \end{vmatrix}. \quad (\text{A18})$$

Calculation of the partial derivatives within the determinant gives

$$h^2 J = \begin{vmatrix} -\cos \theta_s \cos \phi_s + \sin \theta_s S_x & +\sin \theta_s \sin \phi_s \\ -\cos \theta_s \sin \phi_s + \sin \theta_s S_y & -\sin \theta_s \cos \phi_s \end{vmatrix}, \quad (\text{A19})$$

where $h \equiv \cos \theta_s + \cos \theta_r$. When the determinant is evaluated we find

$$\frac{h^2 J}{\sin \theta_s} = \cos \theta_s - \sin \theta_s \{ \sin \phi_s S_y + \cos \phi_s S_x \}. \quad (\text{A20})$$

Substituting equations (A12) and (A13) for the slopes, the expression between braces becomes

$$\{ -(\sin \theta_r \cos(\phi_s - \phi_r) + \sin \theta_s) / h \}. \quad (\text{A21})$$

When (A21) is multiplied by $-\sin \theta_s$ and recast by means of (A16), we have for the second term on the right-hand side of (A20)

$$-\sin \theta_s \{ \} = (h^2 \tan^2 \theta_n + \sin^2 \theta_s - \sin^2 \theta_r) / 2h. \quad (\text{A22})$$

Using $h - \cos \theta_r$ for the first term on the right-hand side of (A20) and using (A22) for the second term on the right hand side of (A20) we arrive at the following expression for the Jacobian:

$$\frac{h^2 J}{\sin \theta_s} = h + \frac{h}{2} \tan^2 \theta_n - \cos \theta_r + \frac{\sin^2 \theta_s - \sin^2 \theta_r}{2h}. \quad (\text{A23})$$

But (A23) can be rewritten as

$$\frac{h^2 J}{\sin \theta_s} = \frac{h}{2} \sec^2 \theta_n + \frac{h^2 - 2h \cos \theta_r + \sin^2 \theta_s - \sin^2 \theta_r}{2h}. \quad (\text{A24})$$

However, the numerator of the last term in (A24) vanishes with the result, after using (A17), that the Jacobian of the transformation from ocean to sky is given by

$$J = \frac{\sin \theta_s \sec^2 \theta_n}{2h} = \frac{\sec \omega \sin \theta_s \sec^3 \theta_n}{4}. \quad (\text{A25})$$

THE JACOBIAN FOR THE TRANSFORMATION BETWEEN SKY AND SUN

When integrating over the solar disk, it is more convenient to use a coordinate system referred to the solar center than a system referred to the zenith. Figure A-5 shows the spherical triangle that connects the two systems. From the law of cosines and the law of sines for this spherical triangle, we have the transformation equations

$$\begin{aligned}\cos\theta_s &= \cos\theta_o \cos\xi + \sin\theta_o \sin\xi \cos\chi \\ \sin(\phi_o - \phi_s) &= \sin\xi \frac{\sin\chi}{\sin\theta_s}\end{aligned}\tag{A26}$$

The Jacobian of the transformation in (A26) is given by

$$J' = \frac{\partial(\theta_s, \phi_s)}{\partial(\xi, \chi)} \equiv \begin{vmatrix} \partial\theta_s/\partial\xi & \partial\theta_s/\partial\chi \\ \partial\phi_s/\partial\xi & \partial\phi_s/\partial\chi \end{vmatrix}.\tag{A27}$$

Calculation of the partial derivatives within the determinant gives

$$m J' = \begin{vmatrix} +\cos\theta_o \sin\xi - \sin\theta_o \cos\xi \cos\chi & +\sin\theta_o \sin\xi \sin\chi \\ -\cos\xi \sin\chi & -\sin\xi \cos\chi \end{vmatrix},\tag{A28}$$

where $m \equiv \sin^2\theta_s \cdot \cos(\phi_o - \phi_s)$. When the determinant on the right-hand side of (A28) is evaluated, we find that

$$m J' = (-\cos\theta_o \sin\xi \cos\chi + \sin\theta_o \cos\xi) \sin\xi.\tag{A29}$$

From the law of cosines for the side θ_s , we have the identity

$$\sin\xi \cos\chi = \frac{\cos\theta_s - \cos\xi \cos\theta_o}{\sin\theta_o},\tag{A30}$$

which can be substituted into (A29) to give

$$m J' = \left\{ \frac{\cos\xi - \cos\theta_s \cos\theta_o}{\sin\theta_o} \right\} \sin\chi.\tag{A31}$$

But the expression within braces in (A31) is equal to $\sin\theta_s \cdot \cos(\phi_o - \phi_s)$ by the law of cosines for the side ξ . Hence, after m is restored (A31) becomes

$$\sin^2\theta_s \cos(\phi_o - \phi_s) J' = \sin\theta_s \cos(\phi_o - \phi_s) \sin\chi\tag{32}$$

or

$$J' = \frac{\sin\chi}{\sin\theta_s}\tag{33}$$

for the Jacobian of the transformation from sky to sun.

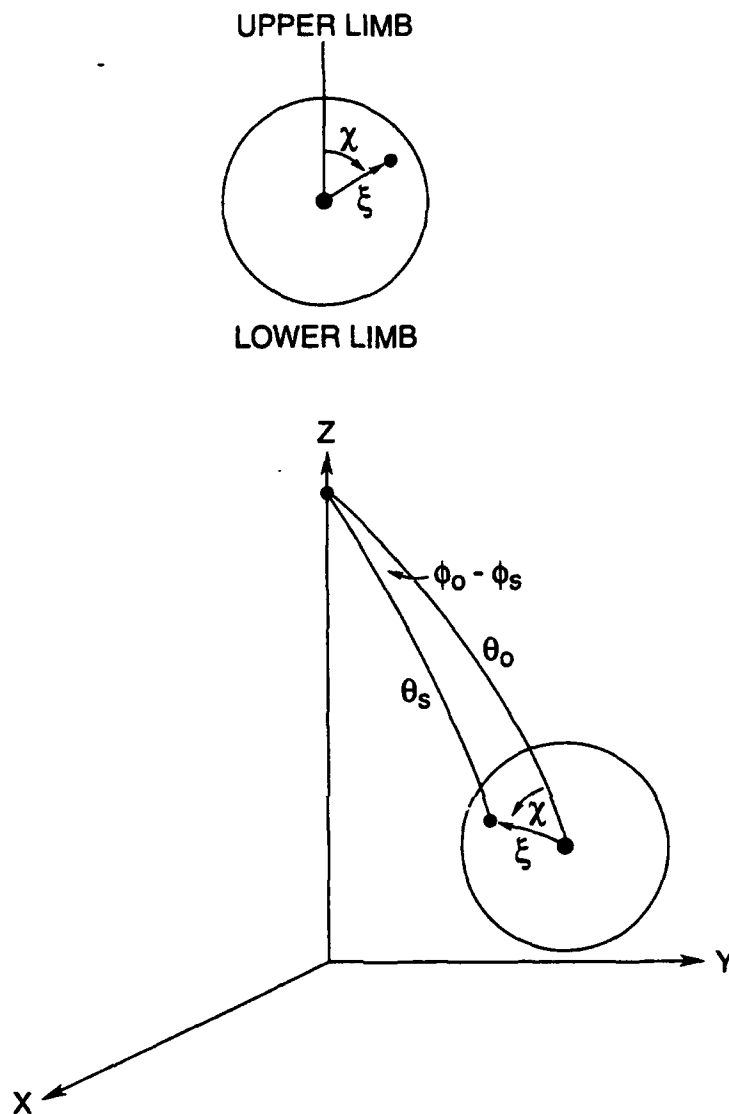


Figure A-5. Upper figure: Coordinates for integration over the solar disk as viewed looking up at the sun from the earth. Lower figure: Spherical triangle connecting the zenith, solar center, and a position on the solar disk as viewed looking down on the sun toward the surface of the earth.

THERMAL EMISSION FROM THE SEA

In the infrared spectral region, solar effects, such as sun glint, become less important and thermal effects, such as black-body emission, become more important. The thermal emission of the sea surface, which is a major component of the infrared radiance of the ocean horizon, will now be derived.

The thermal radiance emitted from a gray surface at absolute temperature T is

$$\epsilon N_*(T) , \quad (A34)$$

where $N_*(T)$ is Planck spectral radiance of a black body

$$N_*(T) = 2c^2h \frac{\nu^3}{\exp(h\nu/kT) - 1} , \quad (A35)$$

and ϵ is the emissivity of the object.² The energy arriving at sea water, an opaque object that does not transmit, can only be reflected or absorbed according to the law of conservation of energy. From Kirchoff's Law, the energy emitted is the same as the energy absorbed. Hence, for sea water

$$\epsilon = 1 - \rho(\omega, \nu) . \quad (A36)$$

We compute the thermal emission arriving at the receiver from the entire footprint shown in figure 9. The logical chain is similar to that given in section 5 of the report; conservation of radiance may not be used directly and the analysis proceeds from the standpoint of power. The thermal power emitted by a facet inside the footprint and captured by the receiver is

$$dP_e = \epsilon N_* \frac{dS}{R^2} dB , \quad (A37)$$

where the quantities dB , dS , and R have previously been defined in section 5 and are also shown in figure 9. Integrating (A37) over all facets and using (7) and (A36) gives

$$P_e = N_* \frac{dS}{R^2} B_r \iint [1 - \rho] q_r dS_x dS_y \quad (A38)$$

for the total power received, which can then be divided by solid angle dS/R^2 and B_r , the area of the rough footprint projected toward the receiver, to give the thermal radiance emitted by the sea:

$$N_e^{sea} = N_*(T_{sea}) \iint [1 - \rho(\omega, \nu)] q_r dS_x dS_y . \quad (A39)$$

² Other symbols in (A35) have their usual meaning.

Equation (A39) represents the thermal emission as an integral over slopes in the ocean. The Jacobian transforming from ocean to sky is $\sin \theta_s \sigma$, where σ is given by (24). Hence,

$$N_e^{sea} = N_*(T_{sea}) \int_0^{\pi/2} d\theta_s \sin \theta_s \int_0^{2\pi} d\phi_s [1 - \rho(\omega, \nu)] q_r \sigma \quad (A40)$$

is an alternate representation for the sea emission in which integration occurs over the sky.

REFERENCES

- Minnaert, M. 1954. *The Nature of Light and Color in the Open Air*, translated by H. M. Kremer-Priest, Dover, NY, pp. 8 ff.
- Saunders, P. 1968. "Radiance of Sea and Sky in the Infrared Window 800–1200 cm^{-1} ," *Journal of the Optical Society of America*, vol. 58, p. 645.
- Cox, C., and W. Munk. 1955. "Some Problems in Optical Oceanography," *Journal of Marine Research*, vol. 14, p. 74.

APPENDIX B
FORTRAN SOURCE CODE LISTINGS

The following FORTRAN programs are based on the equations presented in this report. The equation being computed is noted in columns 73 through 80 of each listing. Each program assembles without errors or warnings on a Lahey F77L/EM-32 compiler version 5.01 and runs on a personal computer provided with a Lahey/Phar Lap 386/DOS-Extender.

These programs accept input from the keyboard and produce output either to the screen or to the hard drive. In the latter case output consists of a file in ASCII format which can be read by commercial software plotting packages. An example of file output follows those listings which created them. Many of the figures in this report were generated with these programs and GRAFTOOL™.

For a copy of this source code on 3 1/2 inch disk please write to the author.

SOURCE CODE

TABLE OF CONTENTS

Functions and Subroutines

Function	Cox-Munk functions.
Rho	Reflectivity of sea water.
Sky	Reflected sky radiance with sea emission.
Sun	Glint radiance ratio.
Tilt	Facet properties.

Plot Drivers

Ellipse	ASCII file for edge of tolerance ellipse.
Plotglnt	ASCII file for glint versus pixel position.
Plotp	ASCII file for p versus slope.
Plotq	ASCII file for q versus slope.
Plotrcvr	ASCII file for glint versus receiver zenith angle.
Plotsun	ASCII file for glint versus solar zenith angle.
Plotwind	ASCII file for glint versus wind speed.

Keyboard Drivers

Testb	Checks function BoverA from keyboard.
Testp	Checks function p from keyboard.
Testq	Checks function q from keyboard.
Testsea	Cox-Munk keyboard and input file driver.
Testsky	Checks "Sky" from keyboard.
Testsun	Checks "Sun" from keyboard.
Testilt	Checks "Tilt" from keyboard.

```

C
***** FUNCTION.FOR *****
*
* Various useful Cox-Munk functions.
*
* Latest revision: August 1, 1994
*
*****
C
FUNCTION Su(W)
C gives the rms upwind slope deviation:
C
C  $Su = \sqrt{3.16E-3 * W}$  (2)
C
C END
C
FUNCTION Sc(W)
C gives the rms crosswind slope deviation:
C
C  $Sc = \sqrt{3.E-3 + 1.92E-3 * W}$  (2)
C
C END
C
FUNCTION p(Sx, Sy, W)
C is the Cox-Munk wave slope probability distribution.
C
COMMON/Constants/Pi, R2D, D2R, Epsilon,
+ Delta, Onem, Onep, Infinity, Zero, T0
C
C  $p0 = 1. / (2. * Pi * Su(W) * Sc(W))$ 
C  $Arg = ((Sx/Su(W))**2 + (Sy/Sc(W))**2) / 2.$ 
C IF ((Arg) .GE. LOG(p0/Delta)) THEN
C     p = Zero
C ELSE
C      $p = p0 * EXP(-Arg)$  (2)
C END IF
C
C END
C
FUNCTION BoverA(Tx, Px, W)
C is area B of the ergodic cap projected toward u = (Tx,Px)
C divided by the area A of the cap projected vertically.
C
C With N = 2, M = 7: Accuracy is < 1% for W below 40 m/s and
C > 1% for W above 40 m/s (due to failure to abandon Cox-Munk
C approximation for the integral above 40 m/s).
C
C Times for a 486 personal computer with a 50 MHz clock:
C Cox-Munk region, 60 microseconds; integral region, 5 milli-
C seconds.
C
COMMON/Constants/Pi, R2D, D2R, Epsilon,
+ Delta, Onem, Onep, Infinity, Zero, T0
C
C N = 2
C M = 7
C
C  $Sav = (Su(W) + Sc(W)) / 2.$ 

```

Smax = N*2.303*Sav
 dS = Smax/M

A = SIN(Tx)*COS(Px) (A2)
 B = SIN(Tx)*SIN(Px)
 C = COS(Tx)

IF (Tx .LE. D2R*58.) THEN (A9)
 BoverA = C (A9)
 ELSE IF ((Tx .LE. D2R*64.) .AND. (W .LE. 26.)) THEN (A9)
 BoverA = C (A9)
 ELSE IF ((Tx .LE. D2R*68.) .AND. (W .LE. 10.)) THEN (A9)
 BoverA = C (A9)
 ELSE IF ((Tx .LE. D2R*72.) .AND. (W .LE. 11.)) THEN (A9)
 BoverA = C (A9)
 ELSE IF ((Tx .LE. D2R*76.) .AND. (W .LE. 6.)) THEN (A9)
 BoverA = C (A9)
 ELSE IF ((Tx .LE. D2R*80.) .AND. (W .LE. 2.)) THEN (A9)
 BoverA = C (A9)
 ELSE
 SUM = 0.
 DO Sx = -Smax, Smax, dS
 Symax = SQRT(ABS(Smax**2 - Sx**2))
 DO Sy = -Symax, Symax, dS
 Ratio = - A*Sx - B*Sy + C (A8)
 IF (Ratio .GT. 0.) SUM = Ratio*p(Sx, Sy, W) + SUM (A7)
 END DO
 END DO
 BoverA = SUM*dS**2
 END IF

END

FUNCTION qo(Tx, Px, Sx, Sy, W)
 is the interaction probability density without "BoverA".

A = SIN(Tx)*COS(Px) (A2)
 B = SIN(Tx)*SIN(Px)
 C = COS(Tx)

Ratio = - A*Sx - B*Sy + C (A8)
 IF (Ratio .GT. 0.) THEN
 qo = Ratio*p(Sx, Sy, W) (13)
 ELSE
 qo = 0. (13)
 END IF

END

FUNCTION q(Tx, Px, Sx, Sy, W)
 is the interaction probability density.

q = qo(Tx, Px, Sx, Sy, W)/BoverA(Tx, Px, W) (13)

END

FUNCTION Ns(a,b,c,T)

```

C      is an analytic form for sky radiance (W m-2 sr-1 (cm-1)-1)
C      as a function of zenith angle T (radians).
C
C      REAL*4 Ns
C
C      Ns = a + b*exp(T/c)
C
C      END
C
C      FUNCTION BB(V, T)
C      is the spectral radiance of a black body in units of
C      W m-2 sr-1 (cm-1)-1. V is the wave number in cm-1 and
C      T is the temperature in Kelvin.
C
C      C1 = 11910.62
C      C2 = 14387.86
C
C      W = 1.E4/V
C      A = C1/W**3
C      X = C2/(W*T)
C
C      BB = A/(Exp(X) - 1.)
C
C      RETURN
C
C      END

```

FUNCTION Rho(Omega, V)

C

COMMON /SeaIndex/ Alpha01(100), Alpha02(20),
+ Beta01 (100), Beta02 (20)

C

***** RHO.FOR *****

*

* Calculates reflectivity of sea water between 52.63 cm-1 and *
* 25,000 cm-1 using equations (74) and (78) of Stratton, "Electro- *
* magnetic Theory", 1941, page 505, ff. The sea water is assumed to *
* be a conducting medium; both real and imaginary parts of the *
* index of water are used. The notation of Stratton is adhered to *
* as closely as possible. *

*

* Omega is the angle of incidence in radians; V is the wave- *
* number in cm-1; Rho is the reflectivity. *

*

* Last revision: March 10, 1994 *

*

C

C The four-point interpolation functions are:

WM(X) = (X - 1.)*(X - 2.)*X/6.

W0(X) = (X - 1.)*(X - 2.)*(X + 1.)/2.

W1(X) = (X + 1.)*(X - 2.)*X/2.

W2(X) = (X + 1.)*(X - 1.)*X/6.

C

IF (V .EQ. 0.) THEN

C

set reflectivity to 100% and return:

Rho = 1.

RETURN

END IF

C

W = 1.E4/V

C

IF (W .LT. 0.399999) THEN

C

print error message and return:

Rho = 0.

WRITE (6, 1000) V

RETURN

END IF

C

IF (0.4 .LE. W .AND. W .LE. 19.8) THEN

C

use Lagrange 4 point interpolation on Block 01 data which

C

are at 0.2 um spacing between 0.2 and 20 um:

I = INT(W/0.2)

Fr = MOD(W, 0.2)/0.2

Alpha1 = W2(Fr)*Alpha01(I + 2) - W1(Fr)*Alpha01(I + 1)

+ W0(Fr)*Alpha01(I) - WM(Fr)*Alpha01(I - 1)

Beta1 = W2(Fr)*Beta01 (I + 2) - W1(Fr)*Beta01 (I + 1)

+ W0(Fr)*Beta01 (I) - WM(Fr)*Beta01 (I - 1)

END IF

C

IF (19.8 .LT. W .AND. W .LT. 190.) THEN

C

use Lagrange 4 point interpolation on Block 02 data which

C

are at 10 um spacing between 10 and 200 um:

I = INT(W/10.)


```

      Fr = MOD(W, 10.)/10.
      Alpha1 = W2(Fr)*Alpha02(I + 2) - W1(Fr)*Alpha02(I + 1)
+      + W0(Fr)*Alpha02(I) - WM(Fr)*Alpha02(I - 1)
      Beta1 = W2(Fr)*Beta02 (I + 2) - W1(Fr)*Beta02 (I + 1)
+      + W0(Fr)*Beta02 (I) - WM(Fr)*Beta02 (I - 1)
      END IF
C
      IF (190. .LE. W) THEN
C      print error message and return:
          RHO = 0.
          WRITE (6, 1000) V
          RETURN
      END IF
C
      G = Alpha1**2 - Beta1**2 - SIN(Omega)**2
      H = 4*(Alpha1**2)*(Beta1**2)
      P = SQRT(0.5*(-G + SQRT(H + G**2)))
      Q = SQRT(0.5*(+G + SQRT(H + G**2)))
C
C      Stratton, Equation (74), p. 505:
C
      C = (Q - COS(Omega))**2 + P**2
      D = (Q + COS(Omega))**2 + P**2
      Rp = C/D
C
C      Stratton, Equation (77), p. 506:
C
      E = ((Alpha1**2 - Beta1**2)*COS(Omega) - Q)**2
      F = ((Alpha1**2 - Beta1**2)*COS(Omega) + Q)**2
      T = (2*Alpha1*Beta1*COS(Omega) - P)**2
      U = (2*Alpha1*Beta1*COS(Omega) + P)**2
      Rs = (E + T)/(F + U)
C
      Rho = (Rp + Rs)/2.
C
      RETURN
C
1000 FORMAT (' ***** WARNING - INPUT FREQUENCY = ', 1PG12.5, 'CM-1',
+          ', ' OUTSIDE VALID RANGE OF 52.63 TO 25,000 CM-1  '*****',/)
C
      END
C
C
C      BLOCK DATA SEA
C
      COMMON /SeaIndex/ Alpha01(100), Alpha02(20),
+          Beta01 (100), Beta02 (20)
C
*****
*
*      These data for the optical index of water have been taken from *
*      the literature. From 0.2 to 2 microns (blocks 01 up to second *
*      entry of row B) and from 10 to 200 microns (blocks 02) the data *
*      are from G. M. Hale and M. R. Querry, "Optical Constants of Water*
*      in the 200-nm to 200-um Wavelength Region," Appl. Opt. 3, 555 *
*      (1973). These data are for pure water. *

```

From 2.2 to 20 microns (blocks 01 from the third entry of row B to the end) the data are from M. R. Querry, W. E. Holland, R. C. Waring, L. M. Earls, and M. D. Querry, "Relative Reflectance and Complex Refractive Index in the Infrared for Saline Environmental Waters," J. Geophys. Res. 82, 1425 (1977), Table 3, Pacific Ocean columns. These data are for salt water.

Real part of the index of sea water from 0.2 to 20 microns in steps of 0.2 microns:

DATA Alpha01 /

A	1.396,	1.339,	1.332,	1.329,	1.327,	1.324,	1.321,	1.317,
B	1.312,	1.306,	1.303,	1.287,	1.251,	1.151,	1.384,	1.479,
C	1.421,	1.388,	1.368,	1.355,	1.347,	1.339,	1.335,	1.335,
D	1.332,	1.324,	1.312,	1.296,	1.268,	1.271,	1.371,	1.353,
E	1.340,	1.330,	1.324,	1.319,	1.314,	1.307,	1.302,	1.297,
F	1.291,	1.286,	1.279,	1.272,	1.268,	1.264,	1.258,	1.249,
G	1.240,	1.229,	1.218,	1.204,	1.190,	1.177,	1.165,	1.151,
H	1.140,	1.132,	1.124,	1.119,	1.121,	1.126,	1.134,	1.142,
I	1.152,	1.164,	1.177,	1.189,	1.201,	1.212,	1.224,	1.234,
J	1.242,	1.253,	1.261,	1.273,	1.284,	1.296,	1.309,	1.320,
K	1.331,	1.339,	1.349,	1.358,	1.366,	1.379,	1.390,	1.399,
L	1.408,	1.417,	1.426,	1.435,	1.443,	1.450,	1.458,	1.464,
M	1.470,	1.474,	1.477,	1.480	/			

Real part of the index of sea water from 10 to 200 microns in steps of 10 microns:

DATA Alpha02 /

A	1.218,	1.480,	1.551,	1.519,	1.587,	1.703,	1.821,	1.886,
B	1.924,	1.957,	1.966,	2.004,	2.036,	2.056,	2.069,	2.081,
C	2.094,	2.107,	2.119,	2.130	/			

Imaginary part of the index of sea water from 0.2 to 20 microns in steps of 0.2 microns:

DATA Beta01 /

A	0.000,	0.000,	0.000,	0.000,	0.000,	0.000,	0.000,	0.000,
B	0.000,	0.001,	0.000,	0.001,	0.003,	0.114,	0.263,	0.085,
C	0.018,	0.005,	0.003,	0.004,	0.007,	0.011,	0.016,	0.016,
D	0.013,	0.011,	0.010,	0.013,	0.032,	0.108,	0.087,	0.044,
E	0.035,	0.033,	0.032,	0.031,	0.031,	0.032,	0.032,	0.033,
F	0.034,	0.036,	0.038,	0.041,	0.044,	0.046,	0.046,	0.047,
G	0.048,	0.050,	0.054,	0.060,	0.068,	0.079,	0.091,	0.107,
H	0.125,	0.145,	0.166,	0.191,	0.216,	0.239,	0.260,	0.279,
I	0.297,	0.313,	0.326,	0.338,	0.347,	0.357,	0.363,	0.371,
J	0.377,	0.385,	0.393,	0.401,	0.407,	0.413,	0.417,	0.418,
K	0.420,	0.422,	0.424,	0.427,	0.430,	0.432,	0.432,	0.432,
L	0.431,	0.430,	0.429,	0.427,	0.425,	0.423,	0.420,	0.416,
M	0.414,	0.410,	0.406,	0.393	/			

Imaginary part of the index of sea water from 10 to 200 microns in steps of 10 microns:

DATA Beta02 /

A	0.051,	0.393,	0.328,	0.385,	0.514,	0.587,	0.576,	0.547,
B	0.536,	0.532,	0.531,	0.526,	0.514,	0.500,	0.495,	0.496,
C	0.497,	0.499,	0.501,	0.504	/			

C

END

SUBROUTINE Sky(V,W,Nsky,Nsea)

C

COMMON/IN/ Ts, Ps, Tr, Pr
 COMMON/OUT/ Sx, Sy, Omega, Tn, Pn
 COMMON/Constants/ Pi, R2D, D2R, Epsilon,
 + Delta, Onem, Onep, Infinity, Zero, T0
 COMMON/Sea/ a, b, c, Tsea

C

***** Sky.FOR *****

* * * * *

* Returns reflected sky radiance Nsky by integrating the source *
 * radiance Ns over the sky dome. Returns emitted sea radiance *
 * Nsea by integrating the sea emission BB over the sky dome. *
 * * * * *

* V is the wavenumber at which reflection occurs and W is the *
 * wind speed at the time of reflection and emission. *
 * * * * *

* USES Function, Tilt, Rho *
 * * * * *

* Latest revision: August 1, 1994 *
 * * * * *

C

REAL*4 Ns, Nsky, Nsea

C

N = 18

C

for 5 degree sky segments and 1% precision.

C

SumSky = 0.

SumSea = 0.

dTs = (Pi/2.)/FLOAT(N)

DO I = 1, N

 Ts = (I - 0.5)*dTs

 K = INT(2.*Pi*Sin(Ts)/dTs + 0.4999)

 dPs = 2*Pi/FLOAT(K)

 SumPsSky = 0.

 SumPsSea = 0.

 DO J = 1, K

 Ps = - Pi + (J - 0.5)*dPs

 CALL Tilt

 SumPsSky =

+ dPs*Rho(Omega,V)/COS(Tn)**4*p(Sx,Sy,W) + SumPsSky (30)

 SumPsSea =

+ dPs*(1 - Rho(Omega,V))/COS(Tn)**4*p(Sx,Sy,W) + SumPsSea (A40)

 END DO

 SumSky = Sin(Ts)*Ns(a,b,c,Ts)*SumPsSky + SumSky (30)

 SumSea = Sin(Ts)*BB(V, Tsea)*SumPsSea + SumSea (A40)

END DO

Nsky = SumSky*dTs/4./BoverA(Tr,Pr,W) (30)

Nsea = SumSea*dTs/4./BoverA(Tr,Pr,W) (A40)

C

RETURN

C

END

SUBROUTINE Sun(V, W, NoverNo)

C

COMMON/IN/ Ts, Ps, Tr, Pr
 COMMON/OUT/ Sx, Sy, Omega, Tn, Pn
 COMMON/Constants/ Pi, R2D, D2R, Epsilon,
 + Delta, Onem, Onep, Infinity, Zero, T0
 COMMON/Sea/ a, b, c, Tsea

C

```
***** Sun.FOR *****
*
* Exact calculation of sun glint ratio N/No. Uses rectangular
* coordinates (x, y) over disk rather than radial coordinates
* (Xi, Chi) given in report.
*
* V is the wavenumber in cm-1, W is the wind speed in m s-1, and
* NoverNo is the glint ratio, an effective reflectivity. This
* subroutine should be called with the common block "IN" loaded
* with Ts, Ps the location of the solar center and Tr, Pr the
* location of the receiver.
*
* The larger the value of M, the y coordinate step size, the more
* precise and slower the sum. For fixed M precision improves
* with wind speed. For W = 1 m s-1 and M = 5, the precision is
* better than 1.5 % around the center of the glint pattern until
* the receiver zenith angle exceeds 89.5 degrees.
*
* USES Tilt, Function, Rho
* Latest revision: August 12, 1994
* Bug: Divides by zero when To = 0 (sun is on the zenith).
```

C

To = Ts
 Po = Ps

C

REAL*4 NoverNo
 M = 5
 N = 2*M + 1

C

```
SUM = 0.
dY = 2.*Epsilon/N
DO I = 1, N
  Y = Epsilon - (I - 0.5)*dY
  Xmax = SQRT(Epsilon**2 - Y**2)
  K = INT(2.*Xmax/dY + Onem*0.5)
  dX = 2.*Xmax/(K)
  DO J = 1, K
    X = Xmax - (J - 0.5)*dX
    Ts = To - Y
    Ps = Po - X/SIN(To)
    CALL Tilt
    SUM = Rho(Omega, V)/(COS(Tn)**4)*p(Sx, Sy, W)*dX + SUM
  END DO
END DO
NoverNo = SUM*dY/Bovera(Tr, Pr, W)/4.
```

C

Ts = To

Ps = Po

C

RETURN

C

END

SUBROUTINE TILT

C

```
COMMON/IN/Ts,Ps,Tr,Pr
COMMON/OUT/Sx,Sy,Omega,Tn,Pn
COMMON/Constants/Pi, R2D, D2R, Epsilon,
+          Delta, Onem, Onep, Infinity, Zero, T0
```

C

```
***** TILT.FOR *****
*
*   Computes various features of facet geometry given the
*   source and receiver coordinates.
*
*   Angles passed in radians.  Azimuths + CCW looking along nadir.
*
*   Latest revision:  August 1, 1994
*
*****
```

C

```
IF ((Ts .GT. Pi/2.*Onep) .OR. (Tn .GT. Pi/2.*Onep)) THEN
    PRINT *, "Error from 'TILT': Zenith angle of source or"
    PRINT *, "                      receiver exceeds 90 degrees."
    RETURN
END IF
```

C

```
As = SIN(Ts)*COS(Ps)          (A2)
Ar = SIN(Tr)*COS(Pr)          .
Bs = SIN(Ts)*SIN(Ps)          .
Br = SIN(Tr)*SIN(Pr)          .
Cs = COS(Ts)                  .
Cr = COS(Tr)                  (A2)
```

C

```
IF (ABS(As + Ar) .LE. Delta) THEN
    Sx = 0.
ELSE IF ((Cs + Cr) .LE. Delta) THEN
    Sx = SIGN(Infinity, -(As + Ar))
ELSE
    Sx = - (As + Ar)/(Cs + Cr)    (A12)
END IF
```

C

```
IF (ABS(Bs + Br) .LE. Delta) THEN
    Sy = 0.
ELSE IF ((Cs + Cr) .LE. Delta) THEN
    Sy = SIGN(Infinity, -(Bs + Br))
ELSE
    Sy = - (Bs + Br)/(Cs + Cr)    (A13)
END IF
```

C

```
D = (1. + As*Ar + Bs*Br + Cs*Cr)/2.    (A14)
IF (D .LE. Delta) D = 0.
S = SQRT (D)                            (A14)
If ((Onem .LE. S) .AND. (S .LE. Onep)) THEN
    Omega = 0.
ELSE IF ((-Onep .LE. S) .AND. (S .LE. -Onem)) THEN
    Omega = Pi
ELSE
    Omega = ACOS(S)                    (A14)
END IF
```

```
C      Tn = ATAN(SQRT(Sx**2 + Sy**2))                                (A6)
C
      IF ((ABS(Sx) .LE. Delta) .AND. (ABS(Sy) .LE. Delta)) THEN
          Pn = 0.
      ELSE IF ((Cs + Cr) .LE. Delta) THEN
          Pn = (Ps + Pr)/2.
      ELSE
          Pn = ATAN2(-Sy, -Sx)                                ! (A2)+(A5)
      END IF
C      RETURN
C      END
```


Plot Drivers

```

COMMON/IN/Ts,Ps,Tr,Pr
COMMON/OUT/Sx,Sy,Omega,Tn,Pn
COMMON/Constants/Pi, R2D, D2R, Epsilon,
+      Delta, Onem, Onep, Infinity, Zero, T0

```

```

C
***** ELLIPSE.FOR *****
*
*   Calculates the Cox-Munk ellipse in slope space such that the
*   slopes within the ellipse will reflect the sun's disk into the
*   receiver. Uses spherical triangle defined by zenith, solar
*   center, and edge of solar disk to compute slopes as the para-
*   meter "Xi" is stepped around the edge of the solar disk. The
*   spherical triangle is shown in figure A-5.
*
*   Computes value of q, the interaction prob. density, for edge
*   of the ellipse and prints it to a file in Sx, Sy, q form for
*   plotting in three dimensions. These data define the edge of
*   the glint cap which is the top of a glint column.
*
*   USES TILT, FUNCTION
*   Last revised: August 1, 1994
*
*****

```

```

C
CHARACTER*80 H
H(1:80) = " "
H(9:11) = "\Sx"
H(23:24) = "Sy"
H(36:36) = "q"
H(44:51) = "Sx - Sxo"
H(58:65) = "Sy - Syo"
H(75:76) = "Xi"

C
Pi      = 4.*ATAN(1.)
R2D     = 180./Pi
D2R     = Pi/180.
Epsilon = D2R*0.2659
Delta   = 1.4E-6
Onem    = 1. - Delta
Onep    = 1. + Delta
Infinity = 999999
Zero    = 0.
T0      = 273.15

```

```

C
IPR = 10
OPEN (IPR, CARriage CONTROL = 'FORTRAN', FILE = 'E.DAT')

```

```

C
PRINT *, "CURRENT WIND SPEED (m s-1) = "
  READ (5, *) W
  IF (W .LT. 0.01) THEN
    W = 0.01
  END IF
PRINT *, "CAMERA ZENITH ANGLE, AZIMUTH (deg) = "
  READ (5, *) Tr, Pr
PRINT *, "SOLAR ZENITH ANGLE, AZIMUTH (deg) = "
  READ (5, *) Tso, Pso

```

```

C

```

```

Tr = D2R*Tr
Pr = D2R*Pr
Tso = D2R*Tso
Pso = D2R*Pso

```

C

```

Ts = Tso
Ps = Pso
CALL TILT
Sxo = Sx
Syo = Sy

```

```

Area= Pi*(Epsilon)**2/(4.*COS(Omega)*COS(Tn)**3) ! (24)+(25)

```

C

```

WRITE (IPR, 90) "\TOLERANCE CAP: WIND SPEED (m/s) = ", W
WRITE (IPR, 80) "\CAMERA ZEN, AZM (deg) = ", R2D*Tr, R2D*Pr
WRITE (IPR, 80) "\SOLAR ZEN, AZM (deg) = ", R2D*Tso, R2D*Pso
WRITE (IPR, 90) "\CENTRAL INCIDENCE ANGLE (deg) = ", R2D*Omega
WRITE (IPR, 90) "\CENTRAL TILT (deg) = ", R2D*Tn
WRITE (IPR, 70) "\APPROXIMATE AREA = ", Area
WRITE (IPR, 60) "\CENTRAL SLOPES Sxo, Syo = ", Sxo, Syo
WRITE (IPR, 20) H

```

C

```

IF ((Tso .GE. Onem*Epsilon) .AND. (Tso .LE. Onep*Epsilon))

```

C

```

    reset zenith angle to value in stable range:

```

```

+   Tso = Tso*Onep

```

```

A = COS(Tso)*COS(Epsilon)

```

```

B = SIN(Tso)*SIN(Epsilon)

```

```

OldC = - Delta

```

```

DO Xi = D2R*0., D2R*360., D2R*10.

```

```

    Ts = ACOS(A + B*COS(Xi))

```

(A26)

```

    C = SIN(Epsilon)/SIN(Ts)*SIN(Xi)

```

(A26)

```

    IF (C .GE. + Onem) C = + Onem

```

```

    IF (C .LE. - Onem) C = - Onem

```

```

    Ps = Pso + ASIN(C)

```

```

    IF (Tso .LT. Onem*Epsilon) THEN

```

```

        zenith pierces solar disk and azimuth cycles + Pi to - Pi:

```

```

        IF ((C .GE. 0.) .AND. (C .GE. OldC)) THEN

```

```

            Ps = - Ps + Pi

```

```

        ELSE IF ((C .LT. 0.) .AND. (C .GE. OldC)) THEN

```

```

            Ps = - Ps - Pi

```

```

        END IF

```

```

    END IF

```

```

    OldC = C

```

```

    CALL TILT

```

```

    WRITE (IPR, 50) Sx, Sy, q(Ts, Ps, Sx, Sy, W),

```

```

+   Sx - Sxo, Sy - Syo, R2D*Xi

```

```

END DO

```

C

```

PRINT *, "DONE. DATA IN 'E.DAT'"

```

C

```

20 FORMAT (A80, /)

```

```

50 FORMAT (2(1PE14.3), 0PF10.3, 2(1PE14.3), 0PF10.0)

```

```

60 FORMAT (A40, 2(1PE15.3), /)

```

```

70 FORMAT (A40, 1PE15.3, /)

```

```

80 FORMAT (A40, 2F9.2, /)

```

```

90 FORMAT (A40, F9.2, /)

```

C

```

END

```

\TOLERANCE CAP: WIND SPEED (m/s) = 10.00
 \CAMERA ZEN, AZM (deg) = 80.00 270.00
 \SOLAR ZEN, AZM (deg) = 80.00 90.00
 \CENTRAL INCIDENCE ANGLE (deg) = 80.00
 \CENTRAL TILT (deg) = 0.00
 \APPROXIMATE AREA = 9.741E-05
 \CENTRAL SLOPES Sxo, Syo = 0.000E+00 0.000E+00

\Sx	Sy	q	Sx - Sxo	Sy - Syo	Xi
0.000E+00	2.320E-03	5.666	0.000E+00	2.320E-03	0.
2.291E-03	2.286E-03	5.667	2.291E-03	2.286E-03	10.
4.515E-03	2.184E-03	5.668	4.515E-03	2.184E-03	20.
6.606E-03	2.017E-03	5.669	6.606E-03	2.017E-03	30.
8.504E-03	1.790E-03	5.672	8.504E-03	1.790E-03	40.
1.015E-02	1.509E-03	5.675	1.015E-02	1.509E-03	50.
1.150E-02	1.183E-03	5.680	1.150E-02	1.183E-03	60.
1.250E-02	8.205E-04	5.686	1.250E-02	8.205E-04	70.
1.313E-02	4.325E-04	5.692	1.313E-02	4.325E-04	80.
1.336E-02	3.055E-05	5.700	1.336E-02	3.055E-05	90.
1.319E-02	-3.733E-04	5.709	1.319E-02	-3.733E-04	100.
1.261E-02	-7.667E-04	5.719	1.261E-02	-7.667E-04	110.
1.165E-02	-1.137E-03	5.729	1.165E-02	-1.137E-03	120.
1.032E-02	-1.474E-03	5.738	1.032E-02	-1.474E-03	130.
8.677E-03	-1.765E-03	5.747	8.677E-03	-1.765E-03	140.
6.758E-03	-2.002E-03	5.755	6.758E-03	-2.002E-03	150.
4.628E-03	-2.177E-03	5.760	4.628E-03	-2.177E-03	160.
2.351E-03	-2.284E-03	5.764	2.351E-03	-2.284E-03	170.
0.000E+00	-2.321E-03	5.765	0.000E+00	-2.321E-03	180.
-2.351E-03	-2.284E-03	5.764	-2.351E-03	-2.284E-03	190.
-4.627E-03	-2.177E-03	5.760	-4.627E-03	-2.177E-03	200.
-6.758E-03	-2.002E-03	5.755	-6.758E-03	-2.002E-03	210.
-8.677E-03	-1.765E-03	5.747	-8.677E-03	-1.765E-03	220.
-1.032E-02	-1.474E-03	5.738	-1.032E-02	-1.474E-03	230.
-1.165E-02	-1.137E-03	5.729	-1.165E-02	-1.137E-03	240.
-1.261E-02	-7.667E-04	5.719	-1.261E-02	-7.667E-04	250.
-1.319E-02	-3.733E-04	5.709	-1.319E-02	-3.733E-04	260.
-1.336E-02	3.055E-05	5.700	-1.336E-02	3.055E-05	270.
-1.313E-02	4.325E-04	5.692	-1.313E-02	4.325E-04	280.
-1.250E-02	8.205E-04	5.686	-1.250E-02	8.205E-04	290.
-1.150E-02	1.183E-03	5.680	-1.150E-02	1.183E-03	300.
-1.015E-02	1.509E-03	5.675	-1.015E-02	1.509E-03	310.
-8.504E-03	1.790E-03	5.672	-8.504E-03	1.790E-03	320.
-6.606E-03	2.017E-03	5.669	-6.606E-03	2.017E-03	330.
-4.514E-03	2.184E-03	5.668	-4.514E-03	2.184E-03	340.
-2.291E-03	2.286E-03	5.667	-2.291E-03	2.286E-03	350.
0.000E+00	2.320E-03	5.666	0.000E+00	2.320E-03	360.

C

```

COMMON/IN/To,Po,Tr,Pr
COMMON/OUT/Sx,Sy,Omega,Tn,Pn
COMMON/Constants/Pi, R2D, D2R, Epsilon,
+      Delta, Onem, Onep, Infinity, Zero, T0

```

C

```

***** PlotGInt.FOR *****
*
*   Plots glint ratio versus receiver elevation and azimuth.
*
*   USES Sun, Tilt, Function, Rho.
*   Last revised: April 26, 1994.
*
*****

```

C

```

Pi      = 4.*ATAN(1.)
R2D     = 180./Pi
D2R     = Pi/180.
Epsilon = D2R*0.2659
Delta   = 1.4E-6
Onem    = 1. - Delta
Onep    = 1. + Delta
Infinity = 999999
Zero    = 0.
T0      = 273.15

```

C

```

REAL*4 NoverNo

```

C

```

IPR = 10
OPEN (IPR, CARRIAGE CONTROL = 'FORTRAN', FILE = 'G.DAT')

```

C

```

PRINT *, "Wind velocity (m s-1) = "
  READ (5, *) W
  IF (W .LE. 0.01) W = 0.01
PRINT *, "Solar Zenith Angle, Azimuth (deg) = "
  READ (5, *) To, Po
  To = D2R*To
  Po = D2R*Po
PRINT *, "Receiver Zenith Angle (deg): Min, Max, Step = "
  READ (5, *) Trmin, Trmax, Trstep
  Trmin = D2R*Trmin
  Trmax = D2R*Trmax
  Trstep = D2R*Trstep
PRINT *, "Receiver Azimuth (deg): Min, Max, Step = "
  READ (5, *) Prmin, Prmax, Prstep
  Prmin = D2R*Prmin
  Prmax = D2R*Prmax
  Prstep = D2R*Prstep
PRINT *, "Wavelength (um) for rho (enter 0. for rho = 100%) = "
  READ (5, *) WL
  IF (WL .EQ. 0.) THEN
    V = 0.
  ELSE
    V = 1.E4/WL
  END IF

```

C

```

WRITE (IPR, 10) "\           A Sun Glint 'Picture': "

```

```

WRITE (IPR, 10) "\                N/No versus Pixel Position"
WRITE (IPR, 50) "\Solar zenith (deg)    = ", R2D*To
WRITE (IPR, 50) "\Solar azimuth (deg)   = ", R2D*Po
WRITE (IPR, 50) "\Wavelength (um)      = ", WL
WRITE (IPR, 50) "\Wind Speed (m s-1)    = ", W
WRITE (IPR, 150)

C
WRITE (IPR, 100) ZERO
DO Tr = Trmin, Onep*Trmax, Trstep
    WRITE (IPR, 100) R2D*Tr
END DO
WRITE (IPR, 150)

C
DO Pr = Prmin, Onep*Prmax, Prstep
    WRITE (IPR, 100) R2D*Pr
    DO Tr = Trmin, Onep*Trmax, Trstep
        CALL Sun(V, W, NoverNo)
        WRITE (IPR, 200) NoverNo
    END DO
    WRITE (IPR, 150)
END DO

C
PRINT *, "DONE.  DATA IN 'G.DAT'."

C
10 FORMAT (A50)
50 FORMAT (/ , A40, F10.2)
100 FORMAT (F10.2, \)
150 FORMAT (/)
200 FORMAT (1PE10.2, \)

C
END

```

\ A Sun Glint 'Picture':
 \ N/No versus Pixel Position

\Solar zenith (deg) = 80.00

\Solar azimuth (deg) = 90.00

\Wavelength (um) = 0.00

\Wind Speed (m s-1) = 10.00

	0.00	76.00	78.00	80.00	82.00	84.00
260.00	3.80E-05	2.82E-05	1.81E-05	9.39E-06	3.55E-06	
262.00	8.99E-05	7.89E-05	6.29E-05	4.42E-05	2.56E-05	
264.00	1.75E-04	1.74E-04	1.65E-04	1.46E-04	1.17E-04	
266.00	2.80E-04	3.06E-04	3.26E-04	3.39E-04	3.42E-04	
268.00	3.72E-04	4.28E-04	4.91E-04	5.62E-04	6.49E-04	
270.00	4.08E-04	4.79E-04	5.62E-04	6.64E-04	8.02E-04	
272.00	3.72E-04	4.28E-04	4.91E-04	5.62E-04	6.49E-04	
274.00	2.80E-04	3.06E-04	3.26E-04	3.39E-04	3.42E-04	
276.00	1.75E-04	1.74E-04	1.65E-04	1.46E-04	1.17E-04	
278.00	8.99E-05	7.89E-05	6.29E-05	4.42E-05	2.56E-05	
280.00	3.81E-05	2.82E-05	1.81E-05	9.39E-06	3.55E-06	

COMMON/Constants/Pi, R2D, D2R, Epsilon,
+ Delta, Onem, Onep, Infinity, Zero, T0

```
C
***** PLOTP.FOR *****
*
*   Calculates Cox-Munk occurrence probability p. Prints p to
*   a file for subsequent graphing on a three dimensional plot.
*
*   USES FUNCTION
*   Last revised: April 22, 1994
*
*****
```

```
C
Pi      = 4.*ATAN(1.)
R2D     = 180./Pi
D2R     = Pi/180.
Epsilon = D2R*0.2659
Delta   = 1.4E-6
Onem    = 1. - Delta
Onep    = 1. + Delta
Infinity = 999999
Zero    = 0.
T0      = 273.15
```

```
C
IPR = 10
OPEN (IPR, CARRIAGE CONTROL = 'FORTRAN', FILE = 'P.DAT')
```

```
C
PRINT *, "CURRENT WIND SPEED (m s-1) = "
  READ (5, *) W
  IF (W .LT. 0.01) THEN
    W = 0.01
  END IF
```

```
PRINT *, "MINIMUM X SLOPE = "
  READ (5, *) Sxmin
PRINT *, "MAXIMUM X SLOPE = "
  READ (5, *) Sxmax
PRINT *, "X SLOPE INCREMENT = "
  READ (5, *) dSx
PRINT *, "MINIMUM Y SLOPE = "
  READ (5, *) Symin
PRINT *, "MAXIMUM Y SLOPE = "
  READ (5, *) Symax
PRINT *, "Y SLOPE INCREMENT = "
  READ (5, *) dSy
```

```
C
WRITE (IPR, 50) "\OCCURRENCE PROB. FOR WIND SPEED = ",
+               W, "M S-1"
```

```
C
WRITE (IPR, 100) ZERO
DO Sy = Symin, Onep*Symax, dSy
  WRITE (IPR, 100) Sy
END DO
WRITE (IPR, 150)
```

```
C
DO Sx = Sxmin, Onep*Sxmax, dSx
  WRITE (IPR, 100) Sx
DO Sy = Symin, Onep*Symax, dSy
```


WRITE (IPR, 200) p(Sx, Sy, W)

END DO

WRITE (IPR, 150)

END DO

C

PRINT *, "DONE. DATA IN 'P.DAT'."

C

50 FORMAT (A40, F6.2, A6, //)

100 FORMAT (F8.4, \)

150 FORMAT (/)

200 FORMAT (F8.2, \)

C

END

\OCCURRENCE PROB. FOR WIND SPEED = 10.00 M S-1

0.0000	-0.2000	-0.1000	0.0000	0.1000	0.2000
-0.2000	1.30	2.55	3.19	2.55	1.30
-0.1000	2.08	4.10	5.13	4.10	2.08
0.0000	2.44	4.80	6.01	4.80	2.44
0.1000	2.08	4.10	5.13	4.10	2.08
0.2000	1.30	2.55	3.19	2.55	1.30

COMMON/Constants/Pi, R2D, D2R, Epsilon,
 + Delta, Onem, Onep, Infinity, Zero, T0

```
C
***** PLOTQ.FOR *****
*
*   Calculates Cox-Munk interaction probability q. Prints q to
*   a file for subsequent graphing on a three dimensional plot.
*
*   USES FUNCTION
*   Last revised: April 4, 1994
**
*****
```

C

```

Pi      = 4.*ATAN(1.)
R2D     = 180./Pi
D2R     = Pi/180.
Epsilon = D2R*0.2659
Delta   = 1.4E-6
Onem    = 1. - Delta
Onep    = 1. + Delta
Infinity = 999999
Zero    = 0.
T0      = 273.15
N       = 2
M       = 7
```

C

```

IPR = 10
OPEN (IPR, CARRIAGE CONTROL = 'FORTRAN', FILE = 'Q.DAT')
```

C

```

PRINT *, "CURRENT WIND SPEED (m s-1) = "
  READ (5, *) W
  IF (W .LT. 0.01) THEN
    W = 0.01
  END IF
PRINT *, "BEAM ZENITH ANGLE (deg) = "
  READ (5, *) T
  T = D2R*T
PRINT *, "BEAM AZIMUTH ANGLE (deg) = "
  READ (5, *) P
  P = D2R*P
PRINT *, "MINIMUM X SLOPE = "
  READ (5, *) Sxmin
PRINT *, "MAXIMUM X SLOPE = "
  READ (5, *) Sxmax
PRINT *, "X SLOPE INCREMENT = "
  READ (5, *) dSx
PRINT *, "MINIMUM Y SLOPE = "
  READ (5, *) Symin
PRINT *, "MAXIMUM Y SLOPE = "
  READ (5, *) Symax
PRINT *, "Y SLOPE INCREMENT = "
  READ (5, *) dSy
```

C

```

WRITE (IPR, 50) "\INTERACTION PROB. FOR WIND SPEED = ",
+               W, "M S-1"
WRITE (IPR, 50) "\ZENITH ANGLE OF BEAM = ",
+               R2D*T, "DEG"
```

```

WRITE (IPR, 50) "\AZIMUTHAL ANGLE OF BEAM = ",
+      R2D*P, "DEG"
WRITE (IPR, 60) "\INTEGRAL = ", BoverA(T,P,W)
WRITE (IPR, 60) "\COS (ZENITH ANGLE) = ", COS(T)
WRITE (IPR, 60) "\INTEGRAL/COS = ", BoverA(T,P,W)/COS(T)
WRITE (IPR, 70) "\N = ", N
WRITE (IPR, 70) "\M = ", M

C
WRITE (IPR, 100) ZERO
DO Sy = Symin, Symax, dSy
    WRITE (IPR, 100) Sy
END DO
WRITE (IPR, 150)

C
DO Sx = Sxmin, Sxmax, dSx
    WRITE (IPR, 100) Sx
    DO Sy = Symin, Symax, dSy
        WRITE (IPR, 200) q(T, P, Sx, Sy, W)
    END DO
    WRITE (IPR, 150)
END DO

C
PRINT *, "DONE.  DATA IN 'Q.DAT'."

C
50 FORMAT (A40, F6.2, A6, //)
60 FORMAT (A40, F9.5, //)
70 FORMAT (A40, I3, //)
100 FORMAT (F8.4, \)
150 FORMAT (/)
200 FORMAT (F8.2, \)

C
END

```

\INTERACTION PROB. FOR WIND SPEED = 10.00 M S-1

\ZENITH ANGLE OF BEAM = 80.00 DEG

\AZIMUTHAL ANGLE OF BEAM = 270.00 DEG

\INTEGRAL = 0.18235

\COS (ZENITH ANGLE) = 0.17365

\INTEGRAL/COS = 1.05014

\N = 2

\M = 7

0.0000	-0.2000	-0.1000	0.0000	0.1000	0.2000
-0.2000	0.00	1.05	3.04	3.80	2.63
-0.1000	0.00	1.69	4.88	6.11	4.23
0.0000	0.00	1.98	5.72	7.16	4.96
0.1000	0.00	1.69	4.88	6.11	4.23
0.2000	0.00	1.05	3.04	3.80	2.63

C

```
COMMON/IN/To,Po,Tr,Pr
COMMON/OUT/Sx,Sy,Omega,Tn,Pn
COMMON/Constants/Pi, R2D, D2R, Epsilon,
+          Delta, Onem, Onep, Infinity, Zero, T0
```

C

```
***** PlotRcvr.FOR *****
*
*   To plot glint as a function of zenith angle of receiver.
*
*   USES Sun, Tilt, Function, Rho.
*   Latest revision: April 26, 1994
*
*****
```

C

```
Pi      = 4.*ATAN(1.)
R2D     = 180./Pi
D2R     = Pi/180.
Epsilon = D2R*0.2659
Delta   = 1.4E-6
Onem    = 1. - Delta
Onep    = 1. + Delta
Infinity = 999999
Zero    = 0.
T0      = 273.15
```

C

```
REAL*4 NoverNo
```

C

```
IPR = 10
OPEN (IPR, CARRIAGE CONTROL = 'FORTRAN', FILE = 'R.DAT')
```

C

```
PRINT *, "Solar Zenith Angle, Azimuth (deg) = "
  READ (5, *) To, Po
  To = D2R*To
  Po = D2R*Po
PRINT *, "Receiver Zenith Angle (deg): Min, Max, Step = "
  READ (5, *) Trmin, Trmax, Trstep
  Trmin = D2R*Trmin
  Trmax = D2R*Trmax
  Trstep = D2R*Trstep
PRINT *, "Receiver Azimuth (deg) = "
  READ (5, *) Pr
  Pr = D2R*Pr
PRINT *, "Wind Speed (m/s) = "
  READ (5, *) W
  IF (W .EQ. 0.) W = 0.01
PRINT *, "Wavelength (um) for rho (enter 0. for rho = 100%) = "
  READ (5, *) WL
  IF (WL .EQ. 0.) THEN
    V = 0.
  ELSE
    V = 1.E4/WL
  END IF
```

C

```
WRITE (IPR, 50) "\Solar zen, az (deg)      = ", R2D*To, R2D*Po
WRITE (IPR, 60) "\Receiver az (deg)        = ", R2D*Pr
WRITE (IPR, 50) "\W (m s-1), Lambda (um) = ", W, WL
```

```

WRITE (IPR, 75)
+" \      Tr (deg)      Nsun/No      Flat-top      Cox-Munk  "
C
DO Tr = Trmin, Trmax, Trstep
  CALL TILT
C    at the solar center to calculate the Cox-Munk glint ratio:
  Gamma = 1./(4.*COS(Tr)*COS(Tn)**4)
  G      = Gamma*Pi*Epsilon**2
  RpG    = Rho(Omega, V)*p(Sx, Sy, W)*G                                (39)
C    and to calculate the flat-top glint ratio:
  Sigma = 1./(4.*COS(Omega)*COS(Tn)**3)                                (24)
  S      = Sigma*Pi*Epsilon**2                                          (25)
  RqS    = Rho(Omega, V)*q(Tr, Pr, Sx, Sy, W)*S                        (35)
C    and then get the actual glint ratio:
  CALL Sun(V, W, NoverNo)
  WRITE (IPR, 100) R2D*Tr, NoverNo, RqS, RpG
END DO
C
50 FORMAT (A35,2F10.2)
60 FORMAT (A35,F20.2)
75 FORMAT (//, A58)
100 FORMAT (F12.2, 3(1PE15.4))
C
PRINT *, "DONE.  DATA IN 'R.DAT'."
C
END

```

\Solar zen, az (deg)	=	80.00	90.00
\Receiver az (deg)	=		270.00
\W (m s-1), Lambda (um)	=	10.00	0.00

\	Tr (deg)	Nsun/No	Flat-top	Cox-Munk
	70.00	2.5603E-04	2.5397E-04	2.5397E-04
	72.00	2.9992E-04	2.9751E-04	2.9751E-04
	74.00	3.4941E-04	3.4663E-04	3.4855E-04
	76.00	4.0810E-04	4.0488E-04	4.0977E-04
	78.00	4.7906E-04	4.7532E-04	4.8583E-04
	80.00	5.6172E-04	5.5740E-04	5.8534E-04
	82.00	6.6431E-04	6.5930E-04	7.2579E-04
	84.00	8.0166E-04	7.9577E-04	9.4837E-04
	86.00	9.6035E-04	9.5358E-04	1.3773E-03
	88.00	1.1692E-03	1.1614E-03	2.6344E-03
	90.00	1.4967E-03	1.4879E-03	-2.1643E+02

C

```
COMMON/IN/To,Po,Tr,Pr
COMMON/OUT/Sx,Sy,Omega,Tn,Pn
COMMON/Constants/Pi, R2D, D2R, Epsilon,
+      Delta, Onem, Onep, Infinity, Zero, T0
```

C

```
***** PlotSun.FOR *****
*
*   To plot glint as a function of solar zenith angle.
*
*   USES Sun, Tilt, Function, Rho.
*   Latest revision: April 26, 1994
*
*****
```

C

```
Pi      = 4.*ATAN(1.)
R2D     = 180./Pi
D2R     = Pi/180.
Epsilon = D2R*0.2659
Delta   = 1.4E-6
Onem    = 1. - Delta
Onep    = 1. + Delta
Infinity = 999999
Zero    = 0.
T0      = 273.15
```

C

```
REAL*4 NoverNo
```

C

```
IPR = 10
OPEN (IPR, CARRIAGE CONTROL = 'FORTRAN', FILE = 'S.DAT')
```

C

```
PRINT *, "Solar Zenith Angle (deg): Min, Max, Step = "
  READ (5, *) Tomin, Tomax, Tostep
  Tomin = D2R*Tomin
  Tomax = D2R*Tomax
  Tostep = D2R*Tostep
PRINT *, "Solar Azimuth (deg) = "
  READ (5, *) Po
  Po = D2R*Po
PRINT *, "Receiver Zenith Angle, Azimuth (deg) = "
  READ (5, *) Tr, Pr
  Tr = D2R*Tr
  Pr = D2R*Pr
PRINT *, "Wind Speed (m/s) = "
  READ (5, *) W
  IF (W .EQ. 0.) W = 0.01
PRINT *, "Wavelength (um) for rho (enter 0. for rho = 100%) = "
  READ (5, *) WL
  IF (WL .EQ. 0.) THEN
    V = 0.
  ELSE
    V = 1.E4/WL
  END IF
```

C

```
WRITE (IPR, 50) "\Receiver zen, az (deg) = ", R2D*Tr, R2D*Pr
WRITE (IPR, 60) "\Solar az (deg) = ", R2D*Po
WRITE (IPR, 50) "\W (m s-1), Lambda (um) = ", W, WL
```

```

WRITE (IPR, 75)
+"\      To (deg)      Nsun/No      Flat-top      Cox-Munk  "
C
DO To = Tomin, Tomax, Tostep
  CALL TILT
  at the solar center to calculate the Cox-Munk glint ratio:
  Gamma = 1./(4.*COS(Tr)*COS(Tn)**4)
  G      = Gamma*Pi*Epsilon**2                                (39)
  RpG    = Rho(Omega, V)*p(Sx, Sy, W)*G
C
  and to calculate the flat-top glint ratio:
  Sigma = 1./(4.*COS(Omega)*COS(Tn)**3)                        (24)
  S      = Sigma*Pi*Epsilon**2                                (25)
  RqS    = Rho(Omega, V)*q(Tr, Pr, Sx, Sy, W)*S               (35)
C
  and then get the actual glint ratio:
  CALL Sun(V, W, NoverNo)
  WRITE (IPR, 100) R2D*To, NoverNo, RqS, RpG
END DO
C
50 FORMAT (A35,2F10.2)
60 FORMAT (A35,F20.2)
75 FORMAT (//, A58)
100 FORMAT (F12.2, 3(1PE15.4))
C
PRINT *, "DONE.  DATA IN 'S.DAT'."
C
END

```

\Receiver zen, az (deg) = 80.00 270.00
 \Solar az (deg) = 90.00
 \W (m s-1), Lambda (um) = 10.00 0.00

\	To (deg)	Nsun/No	Flat-top	Cox-Munk
	70.00	4.8019E-04	4.7634E-04	5.0022E-04
	71.00	4.9480E-04	4.9084E-04	5.1545E-04
	72.00	5.0822E-04	5.0417E-04	5.2944E-04
	73.00	5.2034E-04	5.1620E-04	5.4208E-04
	74.00	5.3106E-04	5.2684E-04	5.5326E-04
	75.00	5.4028E-04	5.3601E-04	5.6288E-04
	76.00	5.4793E-04	5.4362E-04	5.7088E-04
	77.00	5.5395E-04	5.4961E-04	5.7716E-04
	78.00	5.5828E-04	5.5392E-04	5.8170E-04
	79.00	5.6087E-04	5.5653E-04	5.8443E-04
	80.00	5.6172E-04	5.5740E-04	5.8534E-04
	81.00	5.6081E-04	5.5653E-04	5.8443E-04
	82.00	5.5815E-04	5.5392E-04	5.8170E-04
	83.00	5.5375E-04	5.4961E-04	5.7716E-04
	84.00	5.4766E-04	5.4362E-04	5.7088E-04
	85.00	5.3993E-04	5.3601E-04	5.6288E-04
	86.00	5.3061E-04	5.2684E-04	5.5326E-04
	87.00	5.1979E-04	5.1620E-04	5.4208E-04
	88.00	5.0755E-04	5.0417E-04	5.2944E-04
	89.00	4.9399E-04	4.9084E-04	5.1545E-04
	90.00	4.7886E-04	4.7634E-04	5.0022E-04

C

```
COMMON/IN/To,Po,Tr,Pr
COMMON/OUT/Sx,Sy,Omega,Tn,Pn
COMMON/Constants/Pi, R2D, D2R, Epsilon,
+          Delta, Onem, Onep, Infinity, Zero, T0
```

C

```
***** PlotWind.FOR *****
*
*   To plot glint as a function of wind velocity.
*
*   USES Sun, Tilt, Function, Rho.
*   Latest revision: April 26, 1994
*
*****
```

C

```
Pi      = 4.*ATAN(1.)
R2D     = 180./Pi
D2R     = Pi/180.
Epsilon = D2R*0.2659
Delta   = 1.4E-6
Onem    = 1. - Delta
Onep    = 1. + Delta
Infinity = 999999
Zero    = 0.
T0      = 273.15
```

C

```
REAL*4 NoverNo
```

C

```
IPR = 10
OPEN (IPR, CARRIAGE CONTROL = 'FORTRAN', FILE = 'W.DAT')
```

C

```
PRINT *, "Solar Zenith Angle, Azimuth (deg) = "
  READ (5, *) To, Po
  To = D2R*To
  Po = D2R*Po
PRINT *, "Receiver Zenith Angle, Azimuth (deg) = "
  READ (5, *) Tr, Pr
  Tr = D2R*Tr
  Pr = D2R*Pr
PRINT *, "Wavelength (um) for rho (enter 0. for rho = 100%) = "
  READ (5, *) WL
  IF (WL .EQ. 0.) THEN
    V = 0.
  ELSE
    V = 1.E4/WL
  END IF
PRINT *, "Wind velocity (m s-1):  Min, Max, Step = "
  READ (5, *) Wmin, Wmax, Wstep
  IF (Wmin .EQ. Zero) Wmin = 0.01
```

C

```
WRITE (IPR, 50) "\Solar zen, az (deg) = ", R2D*To, R2D*Po
WRITE (IPR, 50) "\Recvr zen, az (deg) = ", R2D*Tr, R2D*Pr
WRITE (IPR, 60) "\Lambda (um)          = ", WL
WRITE (IPR, 75)
+" \      W (m/s)      Ng/No      Flat Top      Cox-Munk  "
```

C

```
DO W = Wmin, Wmax, Wstep
```

```

CALL TILT
C   at the solar center to calculate the Cox-Munk glint ratio:
Gamma = 1./ (4.*COS(Tr)*COS(Tn)**4)
G      = Gamma*Pi*Epsilon**2
RpG    = Rho(Omega, V)*p(Sx, Sy, W)*G           (39)
C   and to calculate the approximate glint ratio:
Sigma = 1./ (4.*COS(Omega)*COS(Tn)**3)           (24)
S      = Sigma*Pi*Epsilon**2                     (25)
RqS    = Rho(Omega, V)*q(Tr, Pr, Sx, Sy, W)*S    (35)
C   and then get the actual glint ratio:
CALL Sun(V, W, NoverNo)
WRITE (IPR, 100) W, NoverNo, RqS, RpG
END DO
C
50 FORMAT (A35,2F10.2)
60 FORMAT (A35,F10.2)
75 FORMAT (//, A58)
100 FORMAT (F12.2, 3(1PE15.4))
C
PRINT *, "DONE.  DATA IN 'W.DAT'."
C
END

```

\Solar zen, az (deg) = 80.00 90.00
 \Recvr zen, az (deg) = 80.00 270.00
 \Lambda (um) = 0.00

\	W (m/s)	Ng/No	Flat Top	Cox-Munk
	1.00	3.9374E-03	3.9319E-03	3.9319E-03
	2.00	2.3696E-03	2.3580E-03	2.3580E-03
	3.00	1.7015E-03	1.6913E-03	1.7013E-03
.	4.00	1.3283E-03	1.3195E-03	1.3344E-03
	5.00	1.0889E-03	1.0813E-03	1.0988E-03
	6.00	9.2206E-04	9.1540E-04	9.3439E-04
.	7.00	7.9852E-04	7.9262E-04	8.1299E-04
	8.00	7.0138E-04	6.9611E-04	7.1962E-04
	9.00	6.2460E-04	6.1984E-04	6.4555E-04
	10.00	5.6172E-04	5.5740E-04	5.8534E-04
	11.00	5.0975E-04	5.0580E-04	5.3543E-04
	12.00	4.6618E-04	4.6254E-04	4.9337E-04
	13.00	4.2916E-04	4.2578E-04	4.5745E-04
	14.00	3.9731E-04	3.9417E-04	4.2642E-04
	15.00	3.6963E-04	3.6670E-04	3.9933E-04
	16.00	3.4532E-04	3.4257E-04	3.7548E-04
	17.00	3.2373E-04	3.2115E-04	3.5432E-04
	18.00	3.0453E-04	3.0209E-04	3.3542E-04
	19.00	2.8735E-04	2.8504E-04	3.1844E-04
	20.00	2.7189E-04	2.6970E-04	3.0309E-04

Keyboard Drivers

COMMON/Constants/Pi, R2D, D2R, Epsilon,
+ Delta, Onem, Onep, Infinity, Zero, T0

```
C
***** TestB.FOR *****
*
*   To display a value of BoverA by entering arguments at the   *
*   keyboard.                                                    *
*
*   USES Function.                                              *
*   Last revised June 6, 1994.                                  *
*
*****
```

```
C
Pi      = 4.*ATAN(1.)
R2D     = 180./Pi
D2R     = Pi/180.
Epsilon = D2R*0.2659
Delta   = 1.4E-6
Onem    = 1. - Delta
Onep    = 1. + Delta
Infinity = 999999
Zero    = 0.
T0      = 273.15
```

```
C
PRINT *, "Beam zenith angle, azimuth (deg) = "
  READ (5, *) T, P
  T = D2R*T
  P = D2R*P
PRINT *, "Wind speed = "
  READ (5, *) W
  IF (W .LT. 0.01) W = 0.01
```

```
C
PRINT *, "BoverA = ", BoverA(T, P, W)
```

```
C
END
```



```
COMMON/Constants/Pi, R2D, D2R, Epsilon,
+          Delta, Onem, Onep, Infinity, Zero, T0
```

```
C
***** TESTP.FOR *****
*
*   To display a value of p by entering arguments at the keyboard.
*
*   USES Function.
*   Last revised 16 March, 1994.
*
*****
```

```
C
Pi      = 4.*ATAN(1.)
R2D     = 180./Pi
D2R     = Pi/180.
Epsilon = D2R*0.2659
Delta   = 1.4E-6
Onem    = 1. - Delta
Onep    = 1. + Delta
Infinity = 999999
Zero    = 0.
T0      = 273.15
```

```
C
PRINT *, "Sx, Sy = "
      READ (5, *) Sx, Sy
PRINT *, "Wind speed = "
      READ (5, *) W
      IF (W .LT. 0.01) W = 0.01
```

```
C
PRINT *, "p = ", p(Sx, Sy, W)
```

```
C
END
```

COMMON/Constants/Pi, R2D, D2R, Epsilon,
+ Delta, Onem, Onep, Infinity, Zero, T0

```
C
***** TestQ.FOR *****
*
*   To display a value of q by entering arguments at the keyboard.
*
*   USES Function
*   Last revised: April 4, 1994
*
*****
C
  PRINT *, "Source zenith, azimuth = "
    READ (5, *) Ts, Ps
    Ts = D2R*Ts
    Ps = D2R*Ps
  PRINT *, "Sx, Sy = "
    READ (5, *) Sx, Sy
  PRINT *, "Wind speed = "
    READ (5, *) W
    IF (W .LT. 0.01) W = 0.01
C
  PRINT *, "q = ", q(Ts, Ps, Sx, Sy, W)
C
  END
```

```

C
COMMON/IN/Ths,Phs,Thr,Phr
COMMON/OUT/Sx,Sy,Omega,Tn,Pn
COMMON/Constants/Pi, R2D, D2R, Epsilon,
+          Delta, Onem, Onep, Infinity, Zero, T0

C
***** TestTilt.FOR *****
*
*   To test Tilt.FOR at the keyboard.
*
*   USES Tilt
*   Latest revision:  March 11, 1994
*
*****

C
Pi          = 4.*ATAN(1.)
R2D         = 180./Pi
D2R         = Pi/180.
Epsilon     = D2R*0.2659
Delta       = 1.4E-6
Onem        = 1. - Delta
Onep        = 1. + Delta
Infinity    = 999999
Zero        = 0.
T0          = 273.15

C
PRINT *, "Source Zenith Angle, Azimuth (deg) "
      READ (5, *) Ts, Ps
      Ths = D2R*Ts
      Phs = D2R*Ps

C
PRINT *, "Receiver Zenith Angle, Azimuth (deg) "
      READ (5, *) Tr, Pr
      Thr = D2R*Tr
      Phr = D2R*Pr

C
CALL Tilt

C
PRINT *, "Sx          = ", Sx, "(Alpha = ", R2D*ATAN(Sx), " deg)"
PRINT *, "-tan*cos = ", -TAN(Tn)*COS(Pn)
PRINT *
PRINT *, "Sy          = ", Sy, "(Beta = ", R2D*ATAN(Sy), " deg)"
PRINT *, "-tan*sin = ", -TAN(Tn)*SIN(Pn)
PRINT *
PRINT *, "Omega       = ", R2D*Omega, " deg"
PRINT *
PRINT *, "Tilt        = ", R2D*Tn, " deg"
PRINT *, "Tilt Az.    = ", R2D*Pn, " deg"

C
END

```

C

```

COMMON/IN/ Ts,Ps,Tr,Pr
COMMON/OUT/ Sx,Sy,Omega,Tn,Pn
COMMON/Constants/ Pi,R2D,D2R,Epsilon,
+          Delta,Onem,Onep,Infinity,Zero,T0
COMMON/Sea/ a,b,c,Tsea

```

C

```

***** TestSea.FOR *****
*
* To test Sky.FOR and Sun.FOR from the keyboard.
*
* USES Sun, Sky, Tilt, Function, Rho, and an input file Sea.In.
* Latest revision: April 26, 1994
*
*****

```

C

```

Pi      = 4.*ATAN(1.)
R2D     = 180./Pi
D2R     = Pi/180.
Epsilon = D2R*0.2659
Delta   = 1.4E-6
Onem    = 1. - Delta
Onep    = 1. + Delta
Infinity = 999999
Zero    = 0.
T0      = 273.15
Tsun    = 5900.

```

C

```

REAL*4 Ns, No, Nsky, Nsea, Nsun, NoverNo

```

C

```

IRD = 15
OPEN (IRD, FILE = 'SEA.IN', STATUS = 'OLD')

```

C

```

PRINT *, "Receiver Zenith Angle, Azimuth (deg) = "
  READ (5, *) Tr, Pr
  Tr = D2R*Tr
  Pr = D2R*Pr
PRINT *, "Wind Speed (m/s) = "
  READ (5, *) W
  IF (W .EQ. 0.) W = 0.01

```

C

```

READ (IRD, 100) V
READ (IRD, 200) Tso, Pso, Tau
  Ts = D2R*Tso
  Ps = D2R*Pso
READ (IRD, 300) a, b, c
READ (IRD, 100) Tsea
  Tsea = Tsea + T0

```

C

```

CALL Sun(V, W, NoverNo)
No = BB(V, Tsun)*Tau
Nsun = NoverNo*No
CALL Sky(V, W, Nsky, Nsea)

```

C

```

PRINT *, "Under the following conditions:"
PRINT *, "      Wind Speed (m/s)      = ", W
PRINT *, "      Receiver zen. (deg) = ", R2D*Tr

```

```

PRINT *, "      Receiver azm. (deg) = ", R2D*Pr
PRINT *, "      Solar zenith (deg) = ", Tso
PRINT *, "      Solar azimuth (deg) = ", Pso
PRINT *, "      Wave Number ((cm-1) = ", V
PRINT *, "      Atmos. Transmission = ", Tau
PRINT *
PRINT *, "      No at top atm. = ", BB(V, Tsun)
PRINT *, "      No at footprint = ", No
PRINT *, "      Ns at zenith = ", Ns(a,b,c,0.)
PRINT *, "      Ns at 80. deg = ", Ns(a,b,c,80.*D2R)
PRINT *, "      Ns at horizon = ", Ns(a,b,c,90.*D2R)
PRINT *, "      N* for sea = ", BB(V,Tsea),
+      " at T(C) = ", Tsea-T0
PRINT *
PRINT *, "the Cox-Munk radiance values are:"
PRINT *, "      Nsun = ", Nsun
PRINT *, "      Nsky = ", Nsky
PRINT *, "      Nsea = ", Nsea
PRINT *
PRINT *, "Note: All radiance values in (W m-2 sr-1 (cm-1)-1)."
```

C

```

100 FORMAT (F10.3)
200 FORMAT (3F10.3)
300 FORMAT (3E10.3)
```

C

END

945.			V (cm-1)	FORMAT F10.3
80.	90.	0.3939	Ts (deg), Ps (deg), Tau	FORMAT 3F10.3
1.1779E-2	5.8410E-5	2.2542E-1	a, b, c (W m-2 sr-1 (cm-1)-1)	FORMAT 3E10.3
15.			Tsea (C)	FORMAT F10.3

This is file "Sea1.In" (Copy to "Sea.In")

With Receiver zenith angle = 80 deg.
 Receiver azimuth = 270 deg.
 Wind speed = 10 m s-1

the output of "TestSea" should be

Nsun = 2.51138E-3 W m-2 sr-1 (cm-1)-1
 Nsky = 6.31824E-3 W m-2 sr-1 (cm-1)-1
 Nsea = 7.09113E-2 W m-2 sr-1 (cm-1)-1

C

```

COMMON/IN/ Ts,Ps,Tr,Pr
COMMON/OUT/ Sx,Sy,Omega,Tn,Pn
COMMON/Constants/ Pi, R2D, D2R, Epsilon,
+           Delta, Onem, Onep, Infinity, Zero, T0
COMMON/Sea/ a, b, c, Tsea

```

C

```

***** TestSky.FOR *****
*
* To test Sky.FOR from the keyboard.
*
* USES Sky, Tilt, Function, Rho.
* Latest revision: May 2, 1994
*
*****

```

C

```

Pi      = 4.*ATAN(1.)
R2D     = 180./Pi
D2R     = Pi/180.
Epsilon = D2R*0.2659
Delta   = 1.4E-6
Onem    = 1. - Delta
Onep    = 1. + Delta
Infinity = 999999
Zero    = 0.
T0      = 273.15

```

C

```

REAL*4 Ns, Nsky, Nsea

```

C

```

a = 1.1779E-2
b = 5.8410E-5
c = 12.915652*D2R
Tsea = T0 + 15.

```

C

```

PRINT *, "Receiver Zenith Angle, Azimuth (deg) = "
  READ (5, *) Tr, Pr
  Tr = D2R*Tr
  Pr = D2R*Pr
PRINT *, "Wind Speed (m/s) = "
  READ (5, *) W
  IF (W .EQ. 0.) W = 0.01
PRINT *, "Wavelength (um) for rho (enter 0. for rho = 100%) = "
  READ (5, *) WL
  IF (WL .EQ. 0.) THEN
    V = 0.
  ELSE
    V = 1.E4/WL
  END IF

```

C

```

CALL Sky(V,W,Nsky,Nsea)

```

C

```

PRINT *
PRINT *, "Ns at zenith      = ", Ns(a,b,c,0.)
PRINT *, "Ns at horizon    = ", Ns(a,b,c,90.*D2R)
PRINT *, "N* for sea       = ", BB(V,Tsea), " at T(K) = ", Tsea
PRINT *
PRINT *, "Nsky              = ", Nsky

```

C:\COX\TESTSKY.FOR 7/14/94

C
PRINT *, "Nsea
END

= ", Nsea

C

```
COMMON/IN/Ts,Ps,Tr,Pr
COMMON/OUT/Sx,Sy,Omega,Tn,Pn
COMMON/Constants/Pi, R2D, D2R, Epsilon,
+          Delta, Onem, Onep, Infinity, Zero, T0
```

C

```
***** TestSun.FOR *****
*
*   To test Sun.FOR from the keyboard.
*
*   USES Sun, Tilt, Function, Rho.
*   Latest revision: April 26, 1994
*
*****
```

C

```
Pi      = 4.*ATAN(1.)
R2D     = 180./Pi
D2R     = Pi/180.
Epsilon = D2R*0.2659
Delta   = 1.4E-6
Onem    = 1. - Delta
Onep    = 1. + Delta
Infinity = 999999
Zero    = 0.
T0      = 273.15
```

C

```
REAL*4 NoverNo
```

C

```
PRINT *, "Solar Zenith Angle, Azimuth (deg) = "
  READ (5, *) Ts, Ps
  Ts = D2R*Ts
  Ps = D2R*Ps
PRINT *, "Receiver Zenith Angle, Azimuth (deg) = "
  READ (5, *) Tr, Pr
  Tr = D2R*Tr
  Pr = D2R*Pr
PRINT *, "Wind Speed (m/s) = "
  READ (5, *) W
  IF (W .EQ. 0.) W = 0.01
PRINT *, "Wavelength (um) for rho (enter 0. for rho = 100%) = "
  READ (5, *) WL
  IF (WL .EQ. 0.) THEN
    V = 0.
  ELSE
    V = 1.E4/WL
  END IF
```

C

```
CALL TILT
```

C

```
at the solar center to calculate the Cox-Munk glint ratio:
```

```
Gamma = 1./(4.*COS(Tr)*COS(Tn)**4) (39)
```

```
G      = Gamma*Pi*Epsilon**2
```

```
RpG    = Rho(Omega, V)*p(Sx,Sy, W)*G (39)
```

C

```
then to calculate the "flat-top" glint ratio:
```

```
Sigma = 1./(4.*COS(Omega)*COS(Tn)**3) (24)
```

```
S      = Sigma*Pi*Epsilon**2 (25)
```

```
RqS    = Rho(Omega, V)*q(Tr, Pr, Sx, Sy, W)*S (35)
```

C

```
and finally to get the exact glint ratio:
```

CALL Sun(V, W, NoverNo)

C

PRINT *

PRINT *, "NoverNo (Exact) = ", NoverNo

PRINT *, "Integrand*Disk (Flat-top) = ", RqS

PRINT *, "Cox-Munk = ", RpG

C

END

INITIAL DISTRIBUTION

Code 0012	Patent Counsel	(1)
Code 0274	Library	(2)
Code 0275	Archive/Stock	(6)
Code 50	H. O. Porter	(1)
Code 54	J. H. Richter	(1)
Code 54	N. M. Vorce	(1)
Code 543	R. A. Paulus	(1)
Code 543	K. D. Anderson	(1)
Code 543	A. E. Barrios	(1)
Code 543	S. G. Batham	(1)
Code 543	C. P. Hattan	(1)
Code 543	H. V. Hitney	(1)
Code 543	D. R. Jensen	(1)
Code 543	G. E. Linden	(1)
Code 543	K. M. Littfin	(1)
Code 543	C. P. McGrath	(1)
Code 543	W. L. Patterson	(1)
Code 543	L. T. Rogers	(1)
Code 543	J. Ward	(1)
Code 543	C. R. Zeisse	(100)
Code 555	S. A. Pappert	(1)
Code 555	M. N. McLandrich	(1)
Code 555	S. A. Miller	(1)
Code 555	D. P. Mullin	(1)
Code 555	C. A. Hewett	(1)
Code 754	G. D. Gilbert	(1)
Code 754	D. K. Forbes	(1)
Code 754	D. B. Law	(1)
Code 754	R. M. Carlson	(1)
Code 754	I. Bendall	(1)
Code 754	E. E. Floren	(1)
Code 844	A. R. King	(1)

Defense Technical Information Center
Alexandria, VA 22304-6145

(4)

Aerodyne Research, Inc.
Billerica, MA 01821-3976

(2)

NCCOSC Washington Liaison Office
Washington, DC 20363-5100

Hughes
Lexington, MA 02173

Center for Naval Analyses
Alexandria, VA 22302-0268

Photon Research Associates, Inc.
La Jolla, CA 92037-1020

**Navy Acquisition, Research and Development
Information Center (NARDIC)
Arlington, VA 22244-5114**

Science and Technology Corporation
Hampton, VA 23666-1340

GIDEP Operations Center
Corona, CA 91718-8000

Scripps Institution of Oceanography
La Jolla, CA 92093-0230

(3)

**Naval Surface Warfare Center
Silver Spring, MD 20903-5000**

Viz Ability, Inc.
Corvallis, OR 97330

**Office of Naval Research
Arlington, VA 22217-5000**

**Jet Propulsion Laboratory
Pasadena, CA 91109-8099**

**Naval Postgraduate School
Monterey, CA 93943-5100**

Michigan Technical University
Houghton, MI 49931-1295

Arete' Associates
Sherman Oaks, CA 91413

Texas A&M University
College Station, TX 77843